Searches for exotics with top with the ATLAS detector at $\sqrt{s} = 8$ TeV

Daniela Paredes

On behalf of ATLAS collaboration

Laboratoire de Physique Corpusculaire de Clermont-Ferrand
Université Blaise Pascal – CNRS/IN2P3

Higgs and BSM Physics at the LHC

Trieste, June 24, 2013

In this talk:

1. **$t\bar{t}$ resonances in the lepton+jets channel** ATLAS-CONF-2013-052 :
   - Topcolor leptophobic Z'.
   - Kaluza-Klein gluons g_{KK}.
2. **Anomalous processes in the same-sign dilepton channel** ATLAS-CONF-2013-051 :
   - Vector-Like-Quarks (VLQ).
   - Same-sign top production (tt).
   - Four top quarks ($t\bar{t}t\bar{t}$):
     - Effective model with 4-tops contact interaction.
     - 2UED/RPP.
     - Sgluon.

Outline

1. Part I: $t\bar{t}$ resonances: lepton+jets
   - Benchmark models
   - Analysis overview
   - Results
2. Part II: anomalous process in the same-sign dilepton channel
   - Signals
   - Analysis overview
   - Results
3. Summary

Benchmark models

Some BSM theories predict new heavy bosons that decay primarily into $t\bar{t}$ pairs.

1. **Topcolor:** introduces a new leptophobic Z-like boson: Z' (arXiv:hep-ph/9911288).
   - Narrow resonance: width 1.2% of the mass.
   - Strong coupling to first and third generation of quarks.

   The model explains the top mass and EWSB.

2. **Randall-Sundrum:** Kaluza-Klein gluons arise in this model (arXiv:hep-ph/0701166).
   - Broad resonance: width 15% of the mass.
   - Strongly coupled to the top quark.

   This model introduces a single warped extra dimension and explains the hierarchy problem.

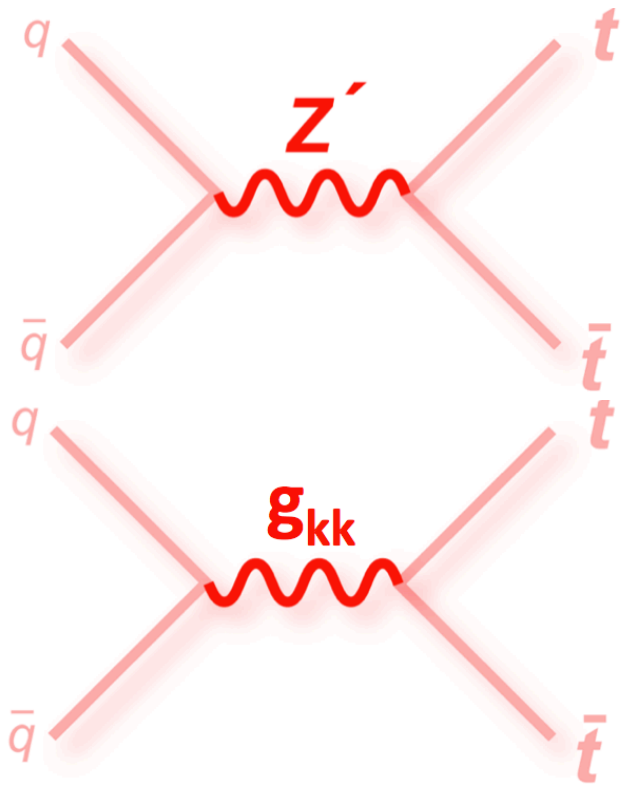

Detector resolution: $\sim$ **7%**

Analysis overview

1. **Data:** collected in 2012 by ATLAS detector @ 8 TeV$\Rightarrow$ 14.3 fb^{-1}.
2. **Background**:
   - SM $t\bar{t}$, $W/Z + jets$, single top and diboson $\Rightarrow$ estimated from MC.
   - $W + jets$ normalization and multijet $\Rightarrow$ estimated from data.
3. **Event selection:** $t\bar{t}$ events are selected in the e or μ+jets channels using two different topologies: boosted and resolved.

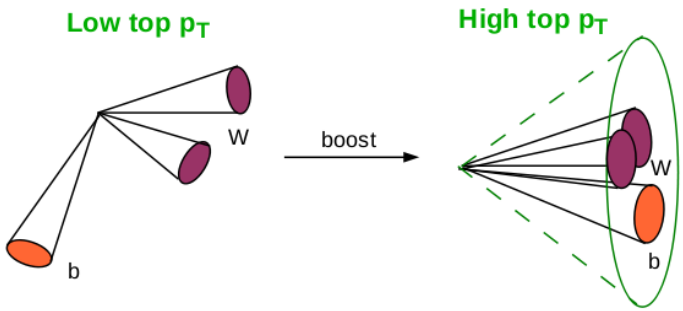

resolved *boosted*

4. **Discriminant variable:** $t\bar{t}$ invariant mass.
5. **Limits:** computed using a Bayesian technique if no excess is found.

Event selection

1 **Lepton selection:** one isolated lepton
- Electron: $E_T > 25$ GeV and $|\eta| < 2.47$.
- Muon: $p_T > 25$ GeV and $|\eta| < 2.5$.

2 **Multijet background rejected by:**
- e **channel:** $E_T^{\text{miss}} > 30$ GeV and $m_T > 30$ GeV with $m_T = \sqrt{2p_T E_T^{\text{miss}}(1 - \cos\Delta\phi)}$.
- μ **channel:** $E_T^{\text{miss}} > 20$ GeV, $E_T^{\text{miss}} + m_T > 60$ GeV.

3 **Jet selection:** **small-radius jets ($R = 0.4$):** $p_T > 25$ **GeV,** $|\eta| < 2.5$.

large-radius jets ($R = 1.0$): $p_T > 300$ **GeV and** $|\eta| < 2.0$.
- **Boosted:** ≥ 1 small-radius jet: highest p_T jet with $\Delta R(\ell, j_{0.4}) < 1.5$.
  ≥ 1 large-radius jet: $m_{jet} > 100$ GeV, $\sqrt{d_{12}} > 40$ GeV, $\Delta R(j_{1.0}, j_{0.4}) > 1.5$ and $\Delta\phi(j_{1.0}, \ell) > 2.3$.
- **OR resolved:** ≥ 4 small-radius jets: $p_T > 25$ GeV, $|\eta| < 2.5$.
  OR ≥ 3 small-radius jets: accepted if $m_{jet} > 60$ GeV for one of these jets.

Resolved topology is applied only if boosted selection failed.

4 ≥ 1 b**-tagged jet.**

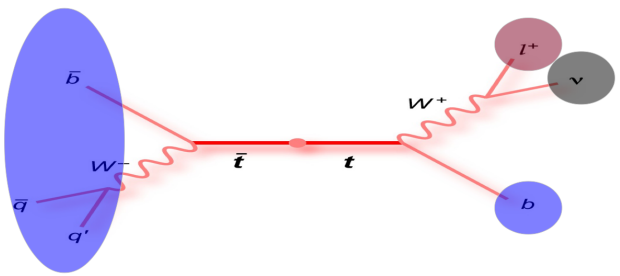

Boosted selection

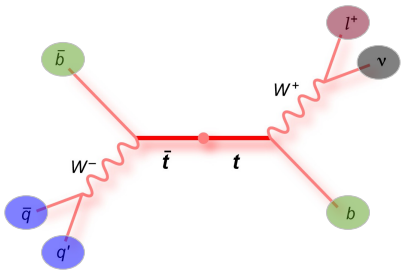

Resolved selection

Data vs. expected background

$t\bar{t}$ invariant mass computed from the four-momenta of the objects in the event.

1. **Resolved:** uses neutrino p_Z and a χ^2 algorithm to select the best assignment to jets.
2. **Boosted:** no ambiguity in the assignment of jets.
   - Hadronic decay $\Rightarrow$ large radius jet.
   - Semi-leptonic decay $\Rightarrow$ Neutrino p_Z, high-p_T lepton and a small radius jet.

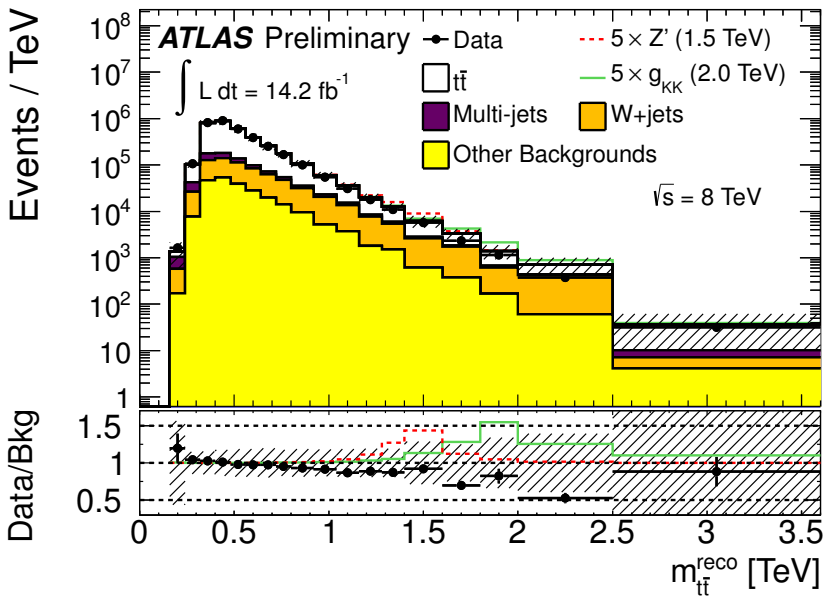

Resolved+boosted

$e+\mu$	Resolved	Boosted
Predicted	283 000 $\pm$ 39 000	5 600 $\pm$ 1 200
Data	280 251	5 122

Observed and expected number of background events

Good agreement between data and expected background within uncertainties

Limits on Z' and g_{KK}

Exclusion ranges @ 95% C.L:

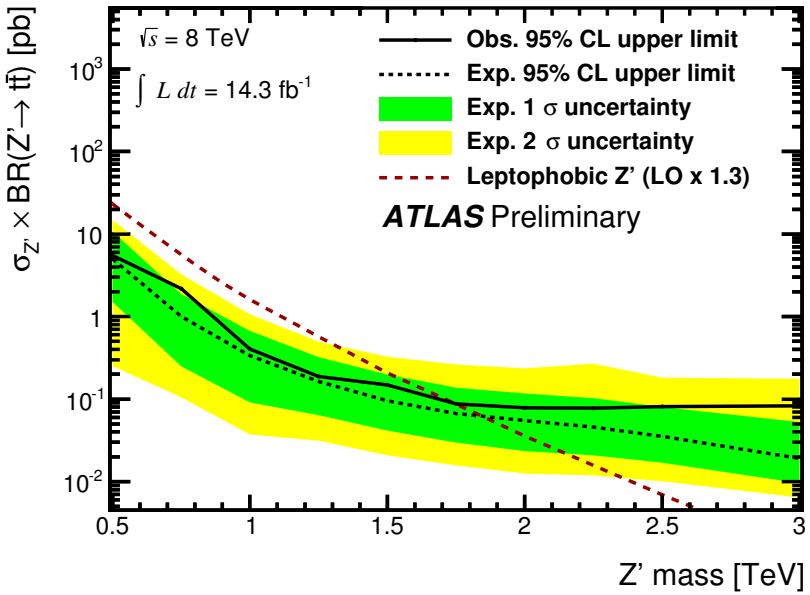

0.5 TeV $< m_{Z'} <$ 1.8 TeV

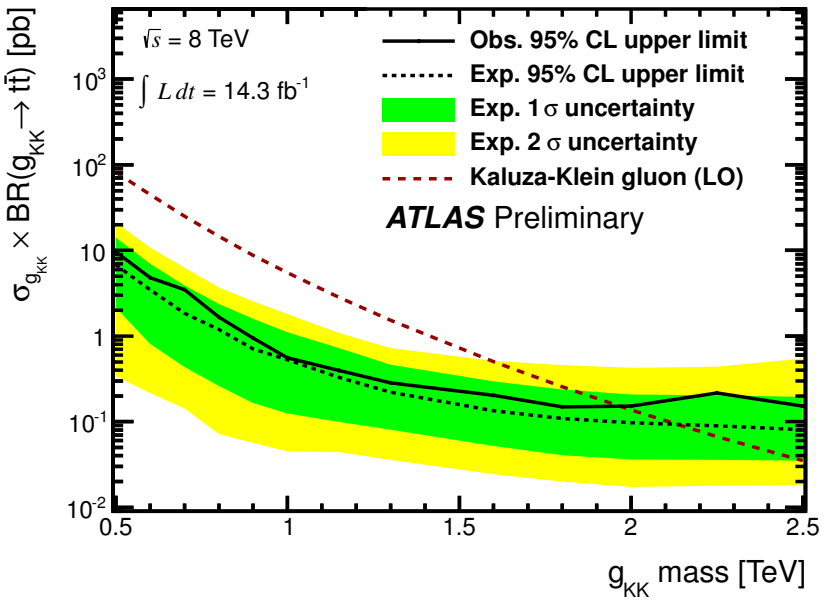

0.5 TeV $< g_{KK} <$ 2.0 TeV

Expected exclusion:
0.5 TeV $< m_{Z'} <$ 1.9 TeV

Expected exclusion:
0.5 TeV $< g_{KK} <$ 2.1 TeV

Outline

Signals: VLQ, tt

1 Vector Like Quarks (VLQ):

- Left- and right-handed components transform identically under $SU(2)_L$.
- Postulated by several extensions of the SM.
  Ex. Partners of SM fermions in Little Higgs Models.
- Considering B and T quarks
  $\Rightarrow B \rightarrow Wt/Zb/Hb$, $T \rightarrow Wb/Zt/Ht$.

Signal indistinguishable from **fourth-generation** $b' \rightarrow Wt$ if BR($B \rightarrow Wt$)=1.

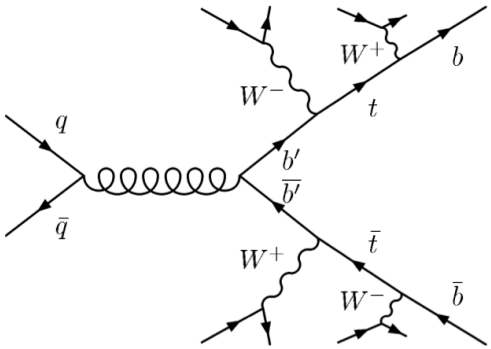

2 Same-sign top:

- Described by an effective four-fermion contact interaction.
- Only $uu \rightarrow tt$ mediated by heavy particle exchange (s-/t-channel).

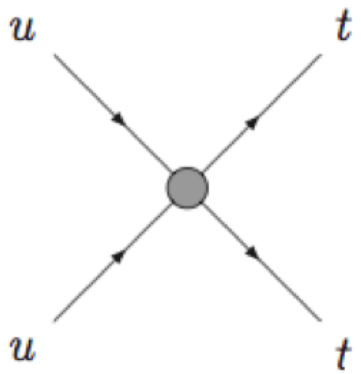

Signal: $t\bar{t}t\bar{t}$

1 Contact interaction:

- $t\bar{t}t\bar{t}$ described by a four top contact interaction.
- Coupling constant C/Λ^2.
- Can test several New Physics theories at low energy.

2 2UED/RPP:

- Model with two universal extra dimensions.
- Predicts pair production of Kaluza-Klein excitations of the photon.

3 Sgluon:

- Color-adjoint scalar.
- Predicted by SUSY models.

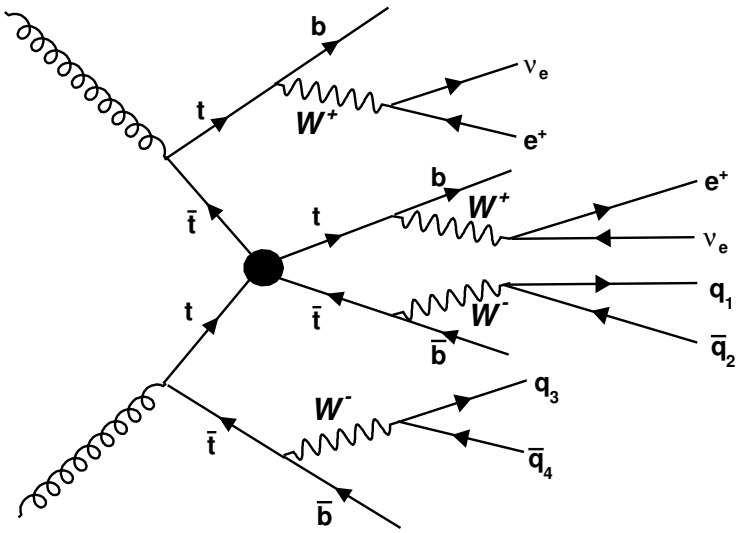

Signal: $t\bar{t}t\bar{t}$

1 Contact interaction:

- $t\bar{t}t\bar{t}$ described by a four top contact interaction.
- Coupling constant C/Λ^2.
- Can test several New Physics theories at low energy.

2 2UED/RPP:

- Model with two universal extra dimensions.
- Predicts pair production of Kaluza-Klein excitations of the photon.

3 Sgluon:

- Color-adjoint scalar.
- Predicted by SUSY models.

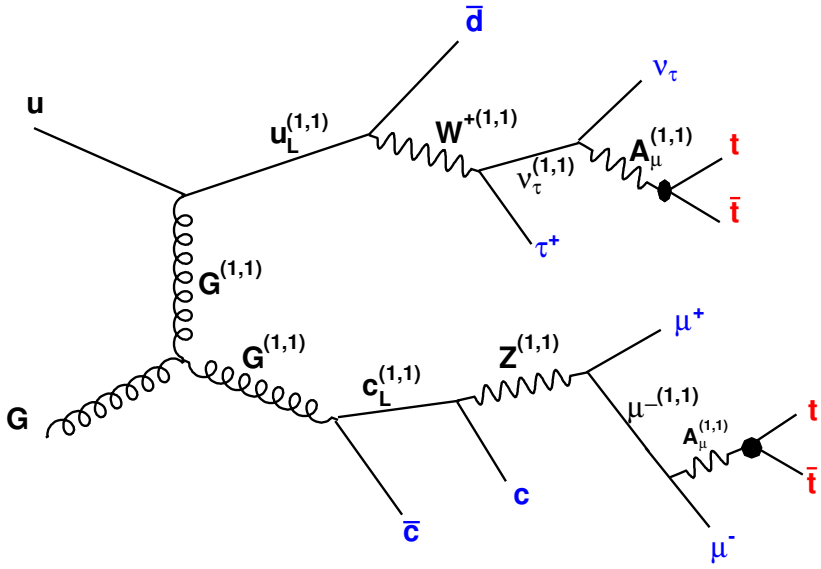

Signal: $t\bar{t}t\bar{t}$

1 Contact interaction:

- $t\bar{t}t\bar{t}$ described by a four top contact interaction.
- Coupling constant C/Λ^2.
- Can test several New Physics theories at low energy.

2 2UED/RPP:

- Model with two universal extra dimensions.
- Predicts pair production of Kaluza-Klein excitations of the photon.

3 Sgluon:

- Color-adjoint scalar.
- Predicted by SUSY models.

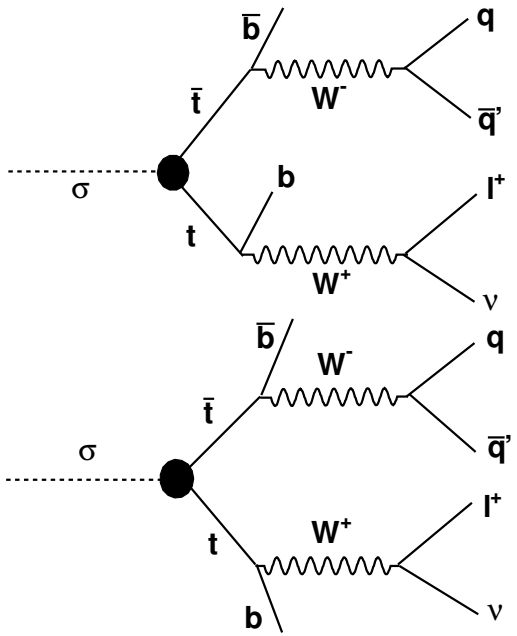

Analysis overview

1. **Data:** collected by ATLAS detector @ 8 TeV $\Rightarrow$ 14.3 fb^{-1}.
2. **Background:**
   - True same sign dilepton pairs: physics processes which give same sign dilepton events $\Rightarrow$ estimated from MC.
   - Instrumental backgrounds: misidentified or misreconstructed objects
     $\rightarrow$ Fakes leptons.
     $\rightarrow$ Electron charge mis-id (negligible for muons).
     $\Rightarrow$Estimated from data
3. **Event preselection:**
   - Two leptons with the same electric charge: $e^{\pm}e^{\pm}$, $e^{\pm}\mu^{\pm}$, $\mu^{\pm}\mu^{\pm}$.
   - Z veto in $e^{\pm}e^{\pm}$ and $\mu^{\pm}\mu^{\pm}$.
   - At least 2 jets, one of them is a b-tagged jet.
   - $E_T^{\mathrm{miss}} > 40$ GeV.
4. **Final selection optimized for each signal:**

Variable	b' and VLQ	tt	$t\bar{t}t\bar{t}$
H_T	$> 650 GeV$	$> 550 GeV$	$> 650 GeV$
N_{b-jets}	≥ 1	≥ 1	≥ 2
Charge	$\pm\pm$	$++$	$\pm\pm$

Summary of the selection for the various signals ($H_T = \sum_{e,\mu,jets} p_T$)

5. **Limits:** computed with CL_S method.

Data and expected background

	Channel					
	ee		$e\mu$		$\mu\mu$	
Signal	Data	Predicted	Data	Predicted.	Data	Predicted
VLQ/b'	3	2.7 ± 0.6	10	4.4 ± 1.0	2	2.3 ± 1.2
$t\bar{t}t\bar{t}$	1	0.75 ± 0.25	6	2.0 ± 0.5	1	0.8 ± 1.2
tt	3	2.5 ± 0.6	8	5.1 ± 1.0	1	3.3 ± 1.1

Expected number of background and observed events after each signal selection

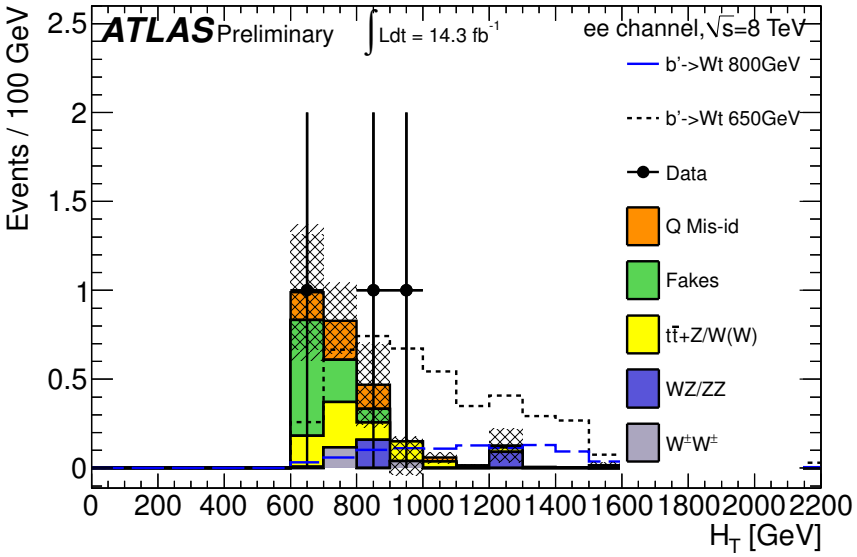

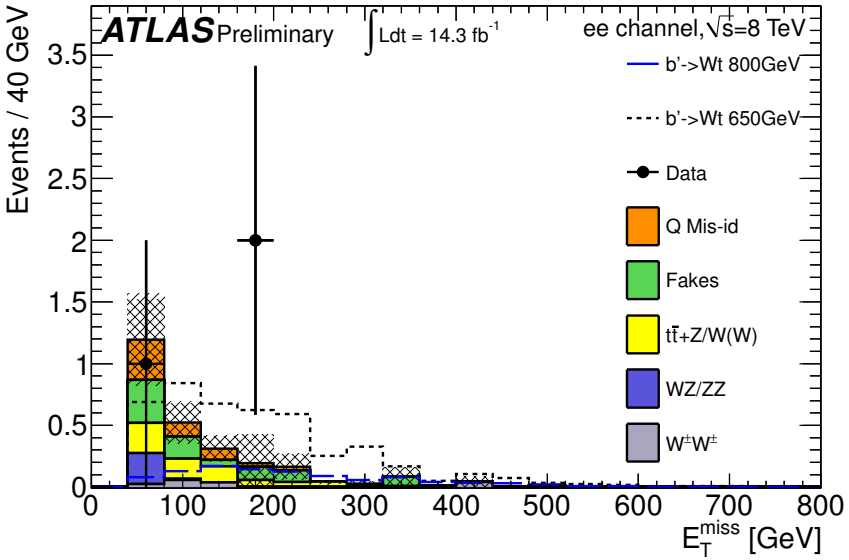

Discriminant variables after VLQ/b' selection

Uncertainties are dominated by the ones coming from the data-driven background and MC production cross-sections

Limits on VLQ mass @ 95% C.L.

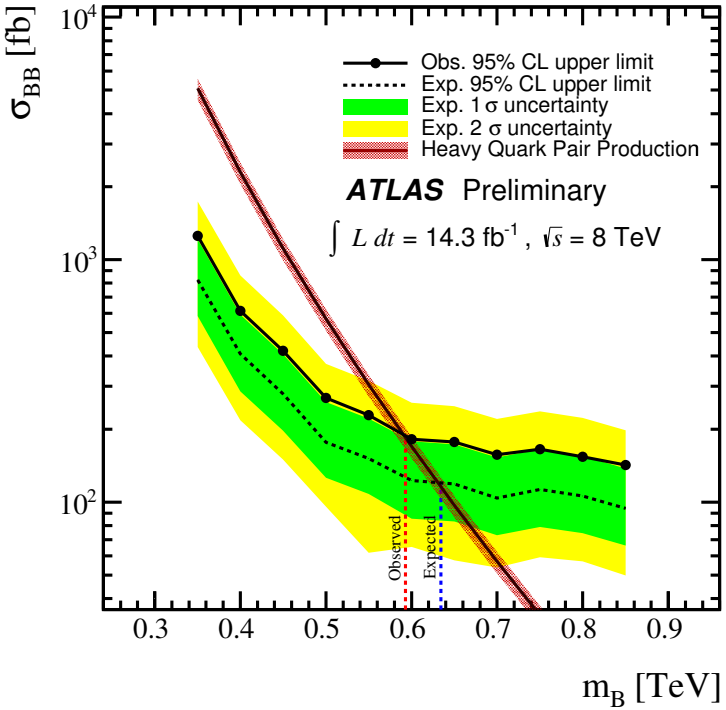

SU(2) singlet: $m_B > 0.59$ **TeV**

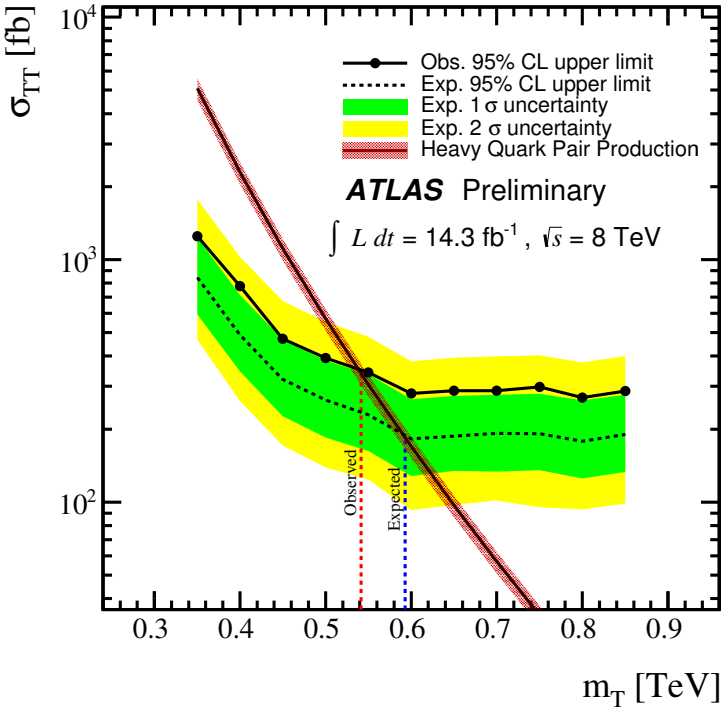

SU(2) singlet: $m_T > 0.54$ **TeV**

Limit on b' mass @ 95% C.L.

Considering $b' \to Wq$ ($q = u, c, t$).

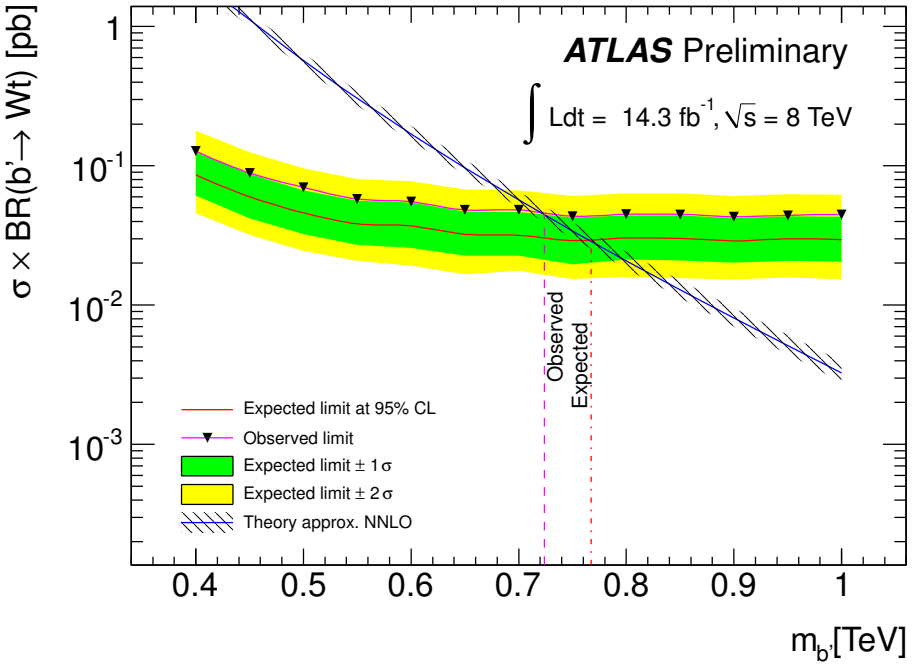

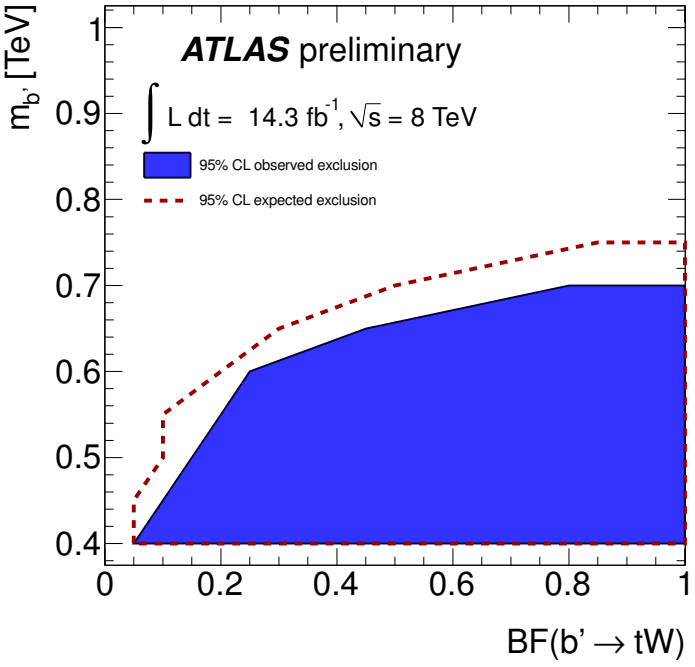

$m_{b'} > 0.72$ **TeV if BR($b' \to Wt$)=1**

Limits on tt production cross-section @ 95% C.L.

	95% C.L. upper limit		
	$\sigma(pp \to tt)$ [pb]		$\lvert C\rvert/\Lambda^2$ [TeV^{-2}]
Chirality configuration	Expected 1σ range	Observed	Observed
Left-left	0.14-0.28	0.19	0.092
Left-right	0.15-0.30	0.20	0.271
Right-right	0.15-0.32	0.21	0.099

Expected and observed limits on the tt pair production signal.

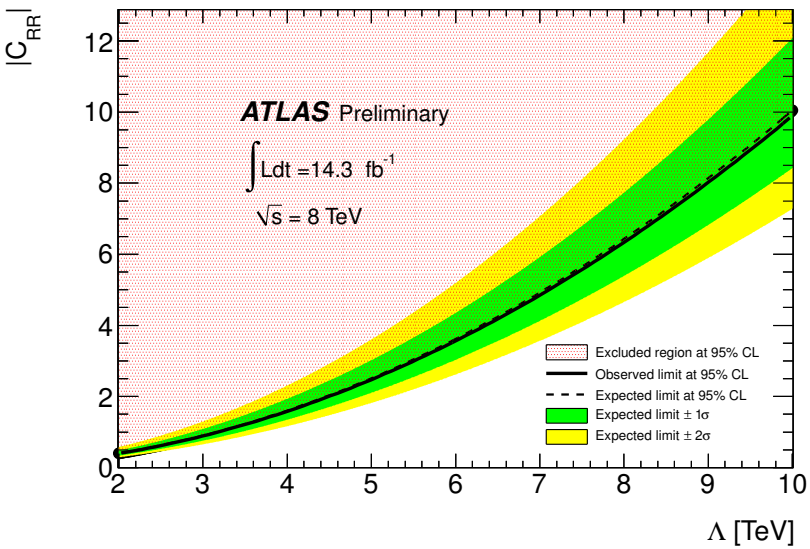

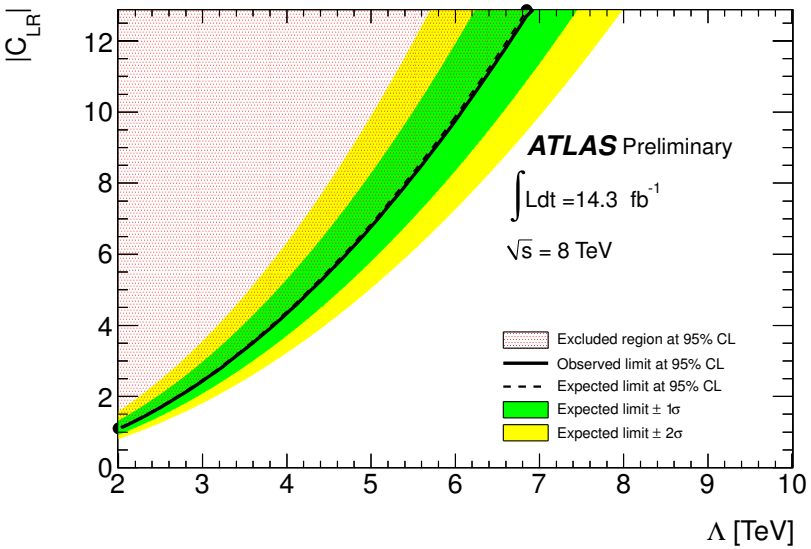

Limit on $t\bar{t}t\bar{t}$ production cross-section @ 95% C.L.

	95% C.L. upper limit		
	$\sigma(pp \to t\bar{t}t\bar{t})$ [fb]		$\lvert C\rvert/\Lambda^2$ [TeV^{-2}]
Model	Expected 1σ range	Observed	Observed
Standard Model	43-89	85	—
Contact interaction	29-61	59	15

Expected and observed limits on two four top quarks signals

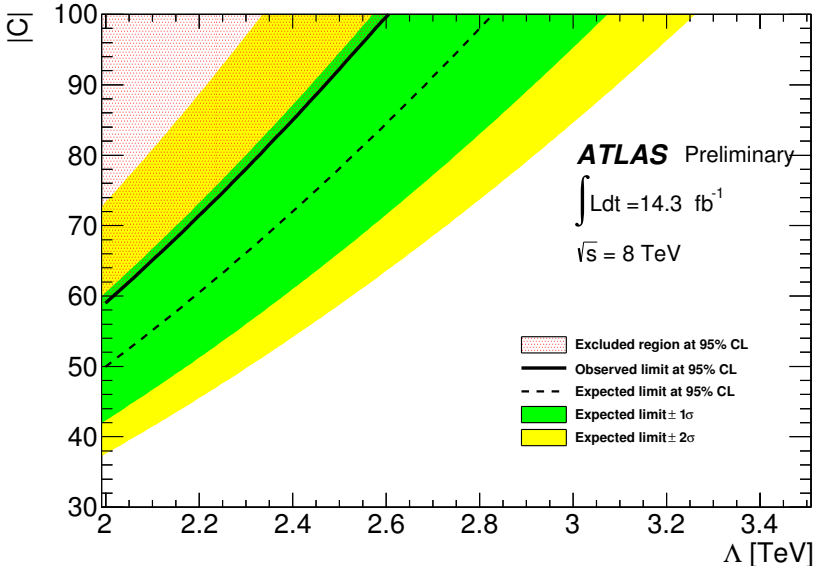

Limit on sgluon and KK mass using $t\bar{t}t\bar{t}$ @ 95% C.L.

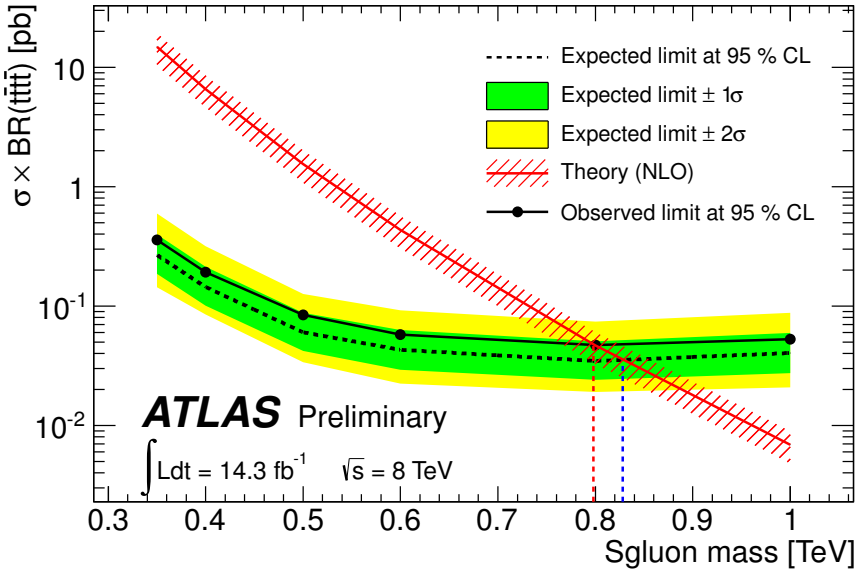

$m_\sigma > 0.80$ **TeV**

,

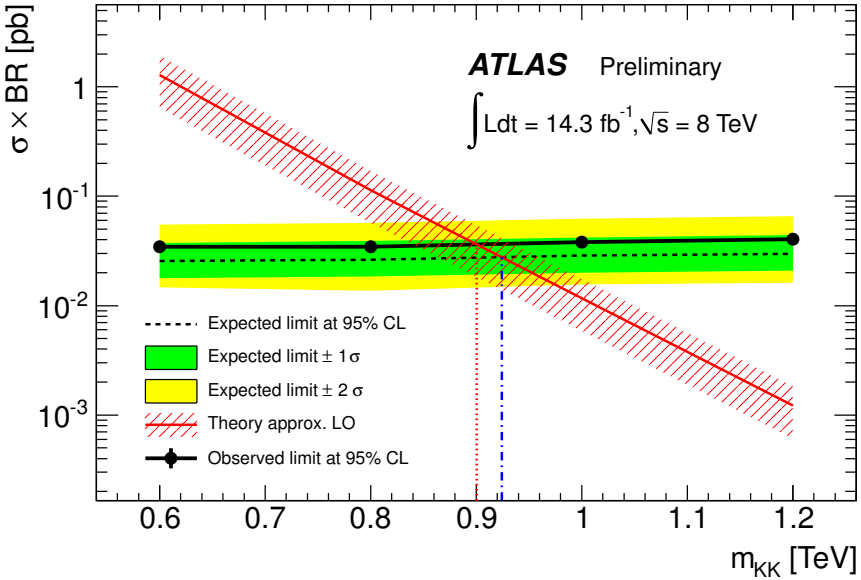

$m_{KK} > 0.90$ **TeV**

Outline

Summary

1. The search for exotic processes in events involving the top quark has been presented: $t\bar{t}$ resonances, b', VLQ, tt and $t\bar{t}t\bar{t}$.
2. No evidence of New Physics has been observed.
3. Limits @ 95% C.L. have been placed.

Signal	Limit
Z'	$m_{Z'} < 0.5$ TeV or $m_{Z'} > 1.8$ TeV
Kaluza-Klein gluons	$g_{KK} < 0.5$ TeV or $g_{KK} > 2.0$ TeV
b'	$m_{b'} > 0.72$ TeV if BR($b' \to Wt$)=1
VLQ (same-sign dilepton)	SU(2) singlet: $m_B > 0.59$ TeV & $m_T > 0.54$ TeV
tt	$\sigma_{LL} < 0.19$ pb, $\sigma_{LR} < 0.20$ pb, $\sigma_{RR} < 0.21$ pb
$t\bar{t}t\bar{t}$ (contact interaction)	$\sigma(pp \to t\bar{t}t\bar{t}) < 59$ fb
Sgluon	$m_\sigma > 0.80$ TeV
Kaluza-Klein mass (2UED/RPP)	$m_{KK} > 0.90$ TeV

4. More results will be obtained with the full 2012 dataset.

BACKUP

$t\bar{t}$ resonances

Triggers

1. Two single muon triggers:
   - $p_T > 24$ GeV with isolation.
   - OR $p_T > 36$ GeV.
2. Two single electron triggers:
   - $p_T > 24$ GeV with isolation.
   - OR $p_T > 60$ GeV.

Samples

1. **SM $t\bar{t}$:** modeled with MC@NLO generator, HERWIG for parton showering and hadronization, and JIMMY for modeling the multiple parton scattering. CT10 PDF are used. $\sigma \times BR = 129$ pb (NNLO).
2. **Single top:**
   - $s-$channel and production with an associated W(Wt) are modeled via MC@NLO/HERWIG/JIMMY with the CT10 PDFs. $\sigma \times BR = 1.8$ pb for s-channel and 22.4 pb for Wt (NNLO).
   - t-channel modeled using ACERMC generator, and PYTHIA for parton showering and hadronization. CTEQ6L1 PDF are used. $\sigma \times BR = 28.4$ pb (NNLO).
3. **$W/Z+$ jets:** generated with ALPGEN with up to 5 extra final state patrons at LO. PYTHIA for parton showering and hadronization. The PDF set used is CTEQ6L1.
4. **Diboson:** modeled with HERWIG and JIMMY with CTEQ6L1 PDFs.
5. **Z':** modeled using the Sequential SM $Z' \rightarrow t\bar{t}$ as implemented in PYTHIA with MSTW2008LO PDFs. The width is $\sim 3\%$ of the mass.
6. **g_{KK}:** generated with MADGRAPH and hadronized with PYTHIA. The width of the resonance is 15.3% of its mass and its branching fraction to $t\bar{t}$ is 92.5%.

$t\bar{t}$ spectrum

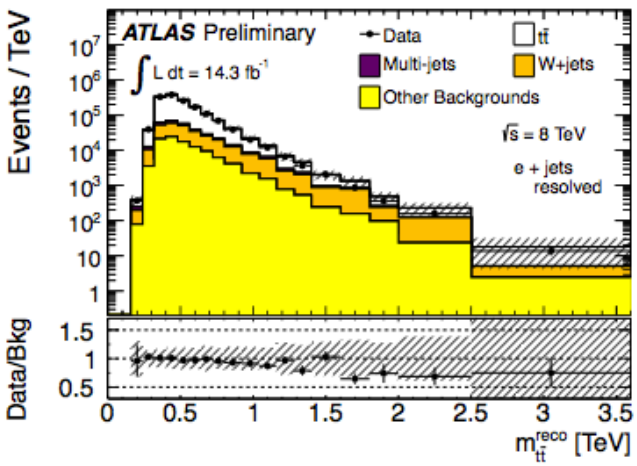

(a) e+jets channel, resolved selection.

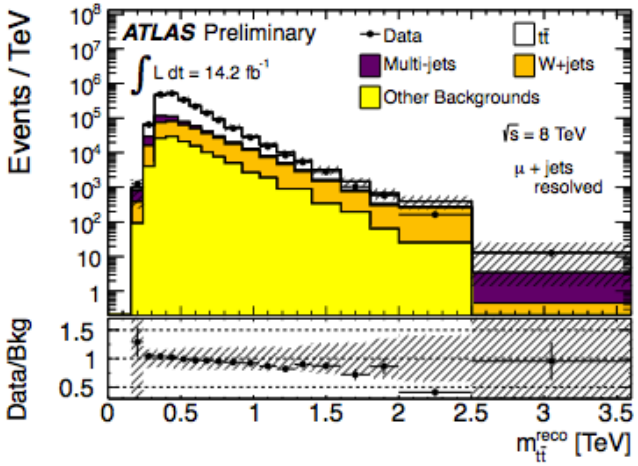

(b) μ+jets channel, resolved selection.

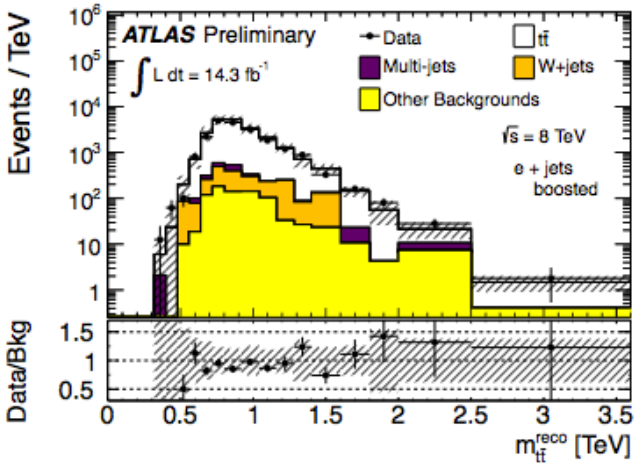

(c) e+jets channel, boosted selection.

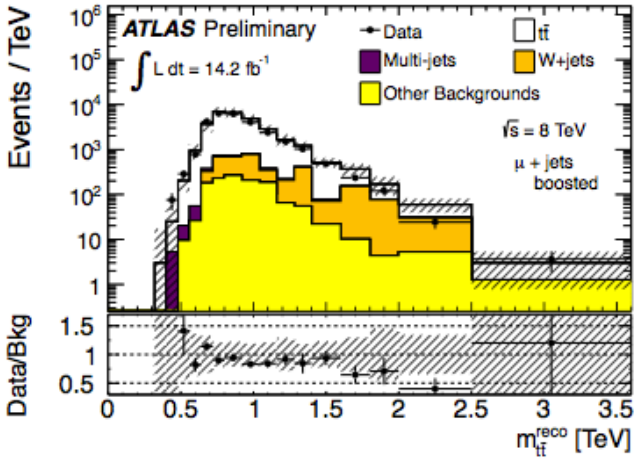

(d) μ+jets channel, boosted selection.

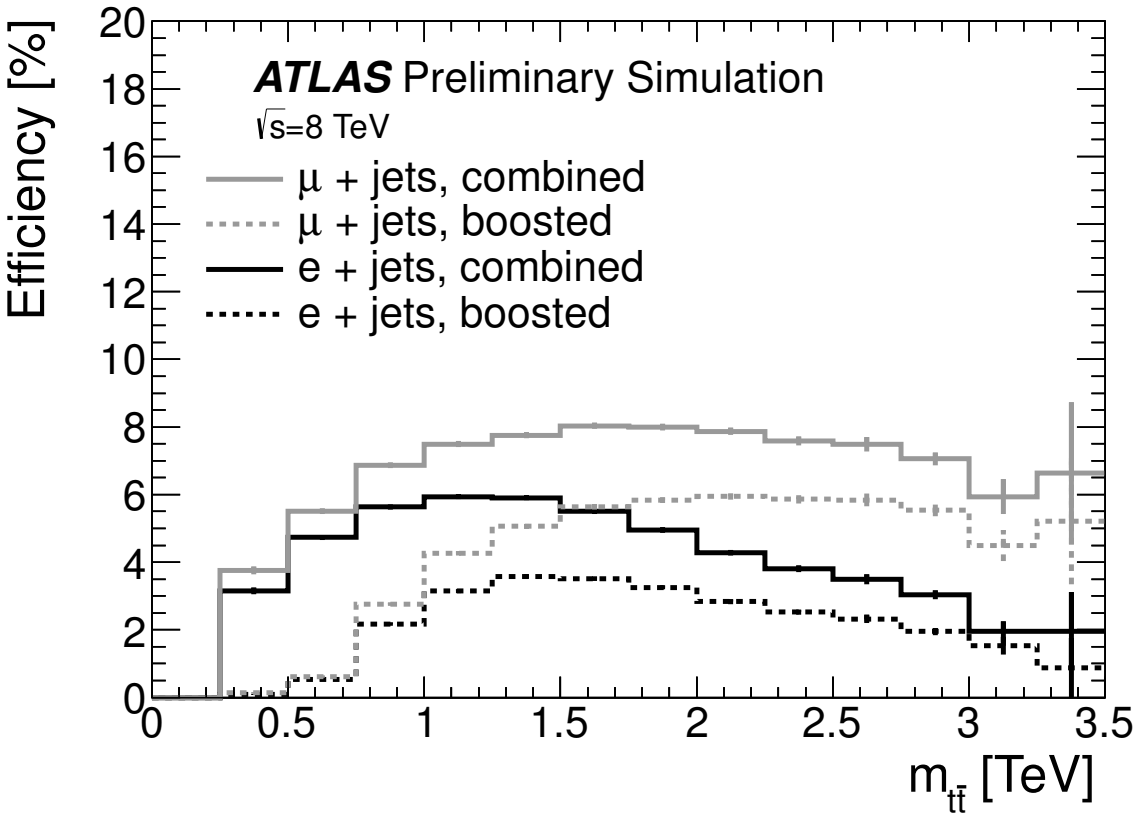

Figure: The selection efficiency at parton level as a function of the true $m_{t\bar{t}}$ for $Z' \to t\bar{t}$ events. The error bars indicate statistical uncertainties.

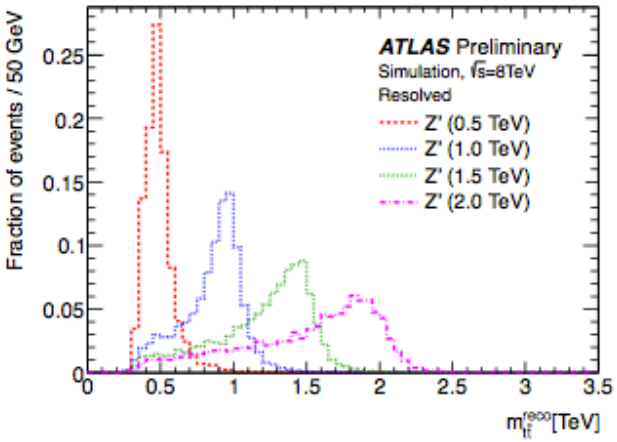

(a) Reconstructed $t\bar{t}$ mass in the resolved selection.

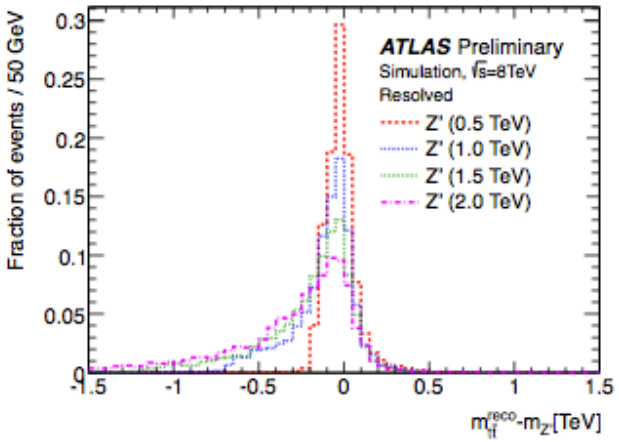

(b) Residuals for the $t\bar{t}$ mass in the resolved selection.

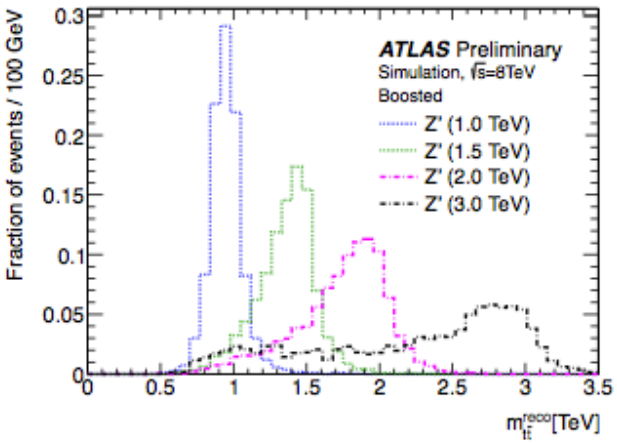

(c) Reconstructed $t\bar{t}$ mass in the boosted selection.

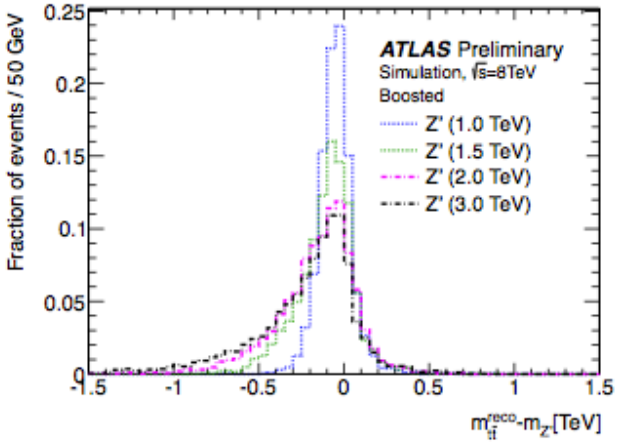

(d) Residuals for the $t\bar{t}$ mass in the boosted selection.

Figure 2: The reconstructed $t\bar{t}$ invariant mass, $m_{t\bar{t}}^{\text{reco}}$, and the corresponding difference between true and reconstructed invariant mass using the resolved (a,b) and boosted selection (c,d), for a range of narrow Z' masses.

Table 1: Average impact of the dominant systematic uncertainties on the total background yield and on the estimated yield of a Z' with $m = 1.5$ TeV. The electron and muon channel spectra are added. The shift is given in percent of the nominal value. Certain systematic uncertainties are not applicable to the Z' samples, which is indicated with a bar (–) in the table.

	Resolved selection yield impact [%]		Boosted selection yield impact [%]	
Systematic Uncertainties	total bkg.	Z'	total bkg.	Z'
Luminosity	2.9	4	3.3	4
PDF	2.9	5	6	2.9
ISR/FSR	0.2	–	0.7	–
Parton shower and fragm.	5	–	4	–
$t\bar{t}$ normalization	8	–	9	–
$t\bar{t}$ EW virtual correction	2.2	–	4	–
$t\bar{t}$ Generator	1.5	–	1.6	–
W+jets $b\bar{b}$+$c\bar{c}$+c vs. light	0.8	–	1.0	–
W+jets $b\bar{b}$ variation	0.2	–	0.4	–
W+jets c variation	1.1	–	0.6	–
W+jets normalization	2.1	–	1.0	–
Multi-Jet norm, e+jets	0.6	–	0.3	–
Multi-Jet norm, μ+jets	1.8	–	0.3	–
JES, small-radius jets	6	2.2	0.7	0.5
JES+JMS, large-radius jets	0.3	4	17	3.3
Jet energy resolution	1.6	0.4	0.6	0.7
Jet vertex fraction	1.7	2.3	2.1	2.4
b-tag efficiency	4	1.8	3.4	6
c-tag efficiency	1.4	0.3	0.7	0.9
Mistag rate	0.7	0.3	0.7	0.1
Electron efficiency	1.0	1.1	1.0	1.0
Muon efficiency	1.5	1.5	1.6	1.6
All systematic uncertainties	14	9	22	9

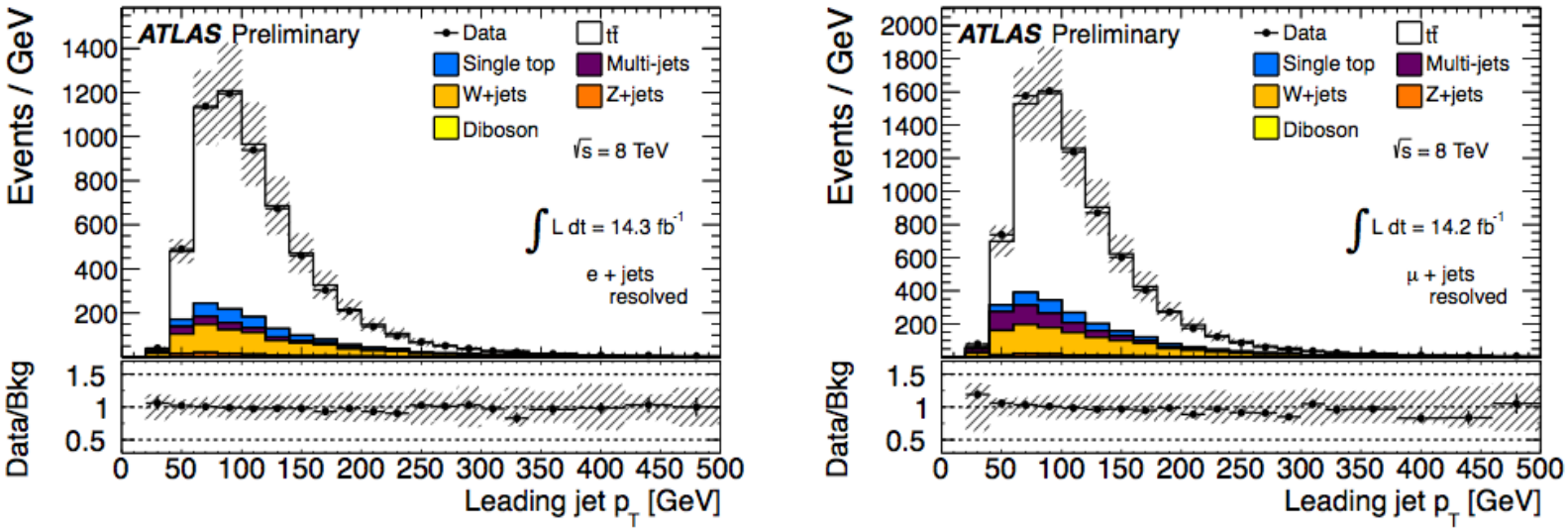

(a) e+jets channel.

(b) μ+jets channel.

Figure 3: The transverse momentum of the leading jet, after the resolved selection. The shaded areas indicate the total systematic uncertainties. Some background sources are too small to be visible in the figure.

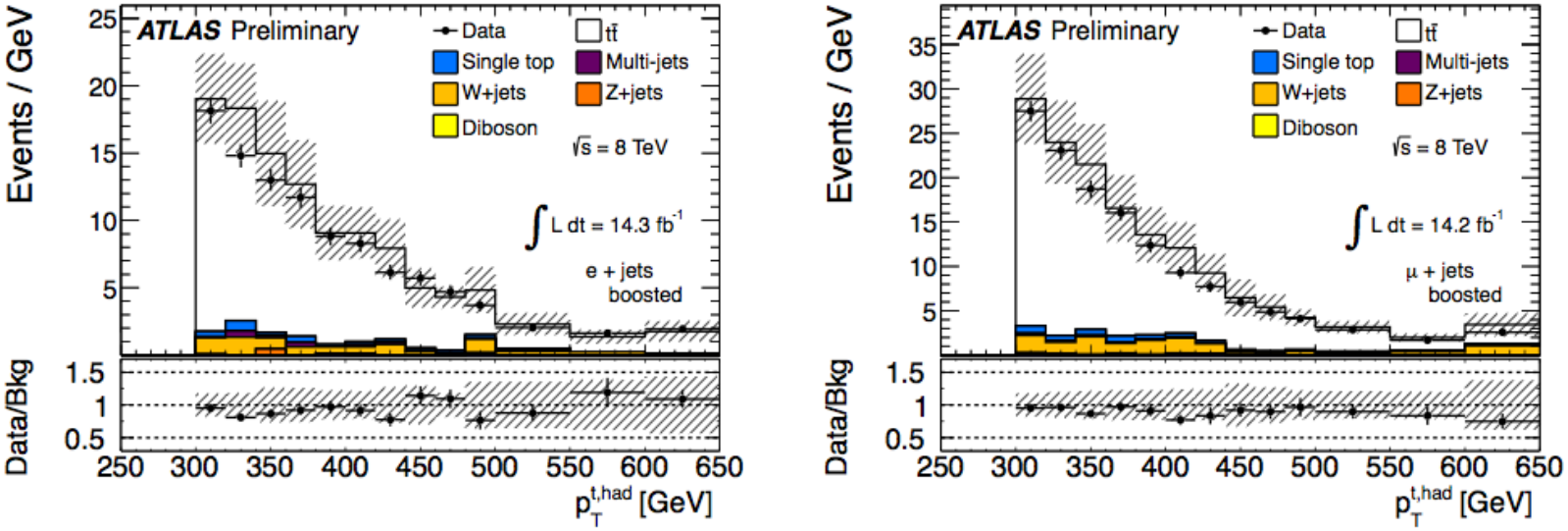

(a) e+jets channel.

(b) μ+jets channel.

Figure 4: The transverse momentum of the hadronically decaying top quark candidate, after the boosted selection. The shaded areas indicate the total systematic uncertainties. Some background sources are too small to be visible in the figure. The last bin in each histogram includes overflow events.

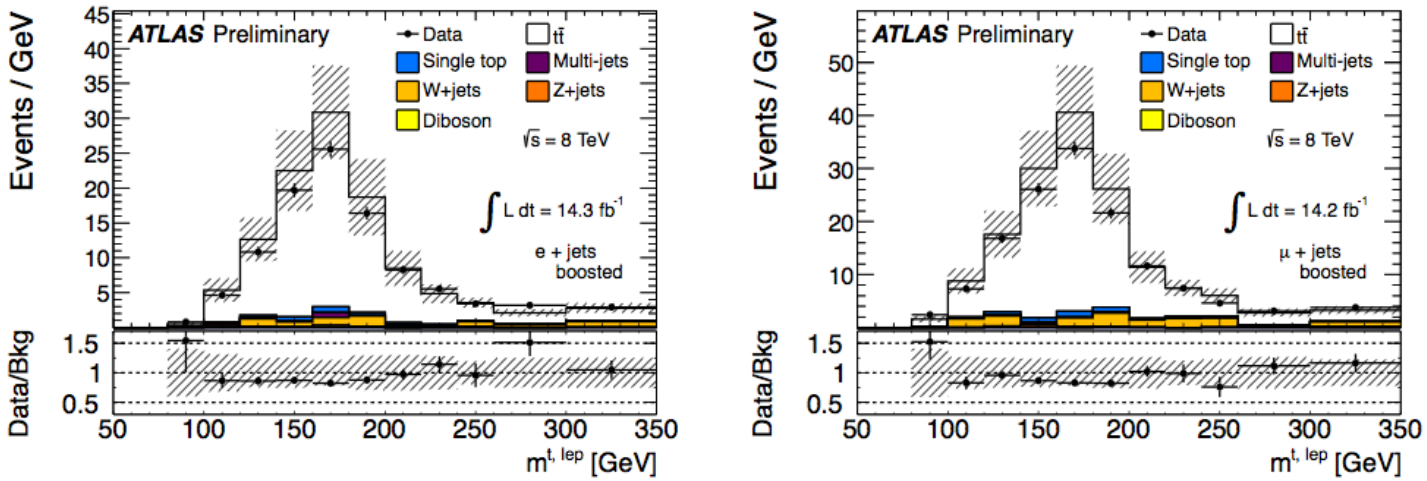

(a) e+jets channel.

(b) μ+jets channel.

Figure 5: The invariant mass of the semi-leptonically decaying top quark candidate, $m^{t,\,\mathrm{lep}}$, after the boosted selection. The mass has been reconstructed from the narrow jet, the charged lepton and the missing transverse momentum, using a W mass constraint to obtain the longitudinal momentum of the neutrino. The shaded areas indicate the total systematic uncertainties. Some background sources are too small to be visible in the figure.

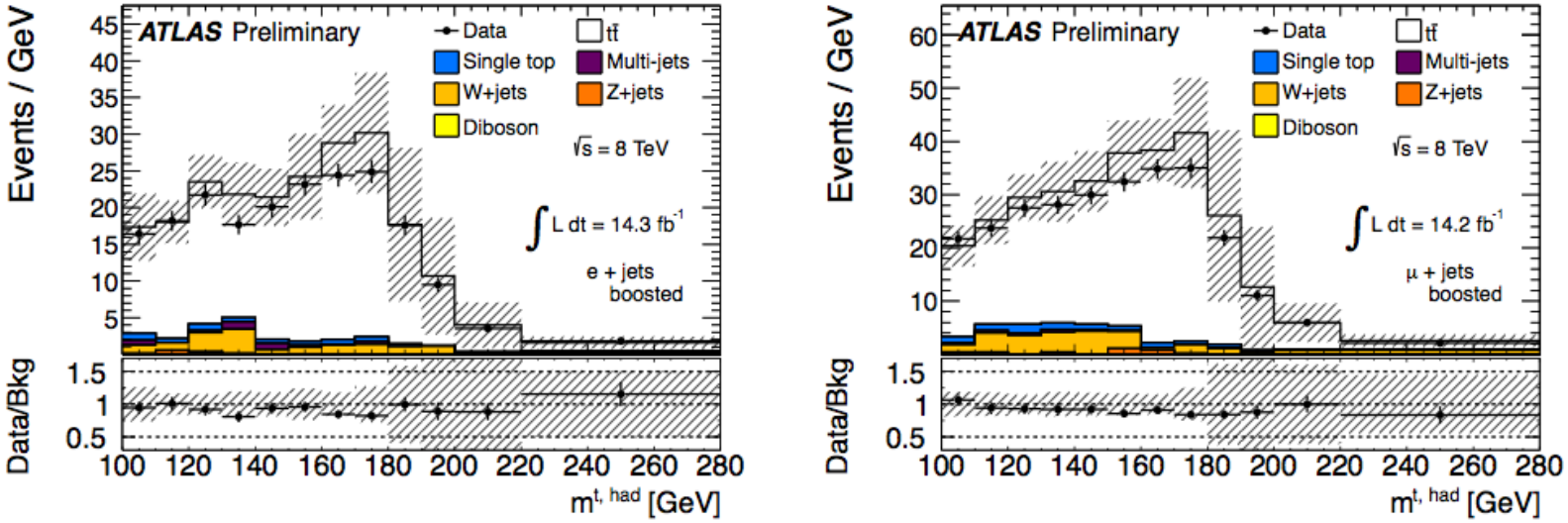

(a) e+jets channel.

(b) μ+jets channel.

Figure 6: The mass of the hadronic top jet, $m^{t,\mathrm{had}}$, after the boosted selection. The shaded areas indicate the total systematic uncertainties. Some background sources are too small to be visible in the figure.

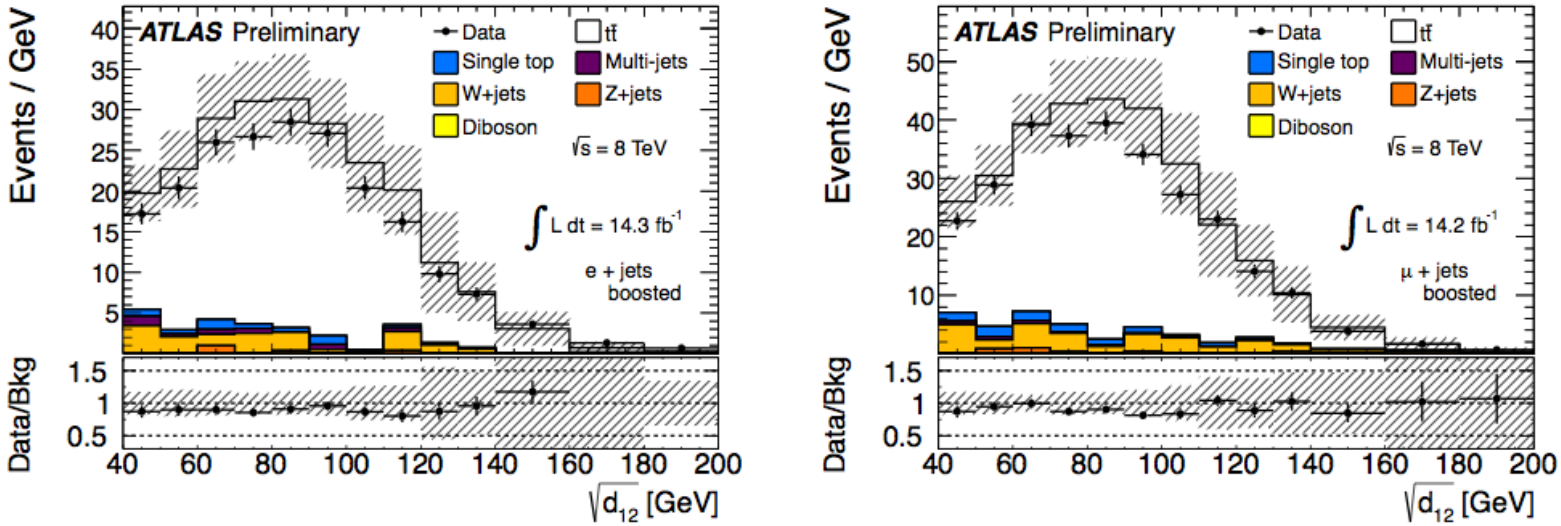

(a) e+jets channel.

(b) μ+jets channel.

Figure 7: The first k_t splitting scale, $\sqrt{d_{12}}$, of the hadronic top jet after the boosted selection. The shaded areas indicate the total systematic uncertainties. Some background sources are too small to be visible in the figure.

Table 2: Data and expected background event yields after the resolved and boosted selections. The uncertainty on the normalization of the expected backgrounds yield is listed.

Resolved selection			
Type	e+jets	μ+jets	Sum
$t\bar{t}$	94000 ± 15000	118000 ± 19000	211000 ± 33000
Single top	6800 ± 800	8400 ± 1100	15200 ± 1900
Multi-jet	3700 ± 1800	10000 ± 5000	14000 ± 6000
W+jets	16000 ± 4000	23000 ± 6000	39000 ± 10000
Z+jets	1800 ± 400	1800 ± 400	3600 ± 800
Di-bosons	230 ± 50	320 ± 60	550 ± 100
Total	121000 ± 17000	162000 ± 23000	283000 ± 39000
Data	119490	160878	280251
Boosted selection			
Type	e+jets	μ+jets	Sum
$t\bar{t}$	2100 ± 500	2800 ± 600	4900 ± 1100
Single top	71 ± 15	105 ± 22	176 ± 34
Multi-jet	39 ± 19	32 ± 16	71 ± 25
W+jets	170 ± 60	310 ± 90	480 ± 140
Z+jets	18 ± 11	33 ± 8	52 ± 15
Di-bosons	2.0 ± 0.8	1.5 ± 1.4	3.5 ± 1.8
Total	2400 ± 500	3300 ± 700	5600 ± 1200
Data	2177	2945	5122

Table 3: Upper 95% CL cross section limits times branching ratio on a leptophobic topcolor Z' decaying to $t\bar{t}$, using the combination of all four samples. The observed and expected limits for each mass point are given, as well as the $\pm 1\sigma$ variation of the expected limit. The second column gives the theoretical predictions with the 1.3 K-factor to account for NLO effects.

Mass (TeV)	$\sigma\times$ BR $\times$1.3 [pb]	Obs. (pb)	Exp. (pb)	-1σ (pb)	$+1\sigma$ (pb)
0.50	23.	5.30	4.99	1.50	10.7
0.75	5.6	2.17	1.00	0.249	1.87
1.00	1.6	0.406	0.335	0.091	0.674
1.25	0.57	0.187	0.160	0.064	0.323
1.50	2.1×10^{-1}	0.148	0.096	0.041	0.198
1.75		0.087	0.066	0.030	0.137
2.00	3.9×10^{-2}	0.078	0.055	0.023	0.117
2.25		0.078	0.045	0.021	0.103
2.50	6.9×10^{-3}	0.081	0.035	0.017	0.081
3.00	1.5×10^{-3}	0.083	0.019	0.010	0.053

Table 4: Upper 95% CL cross section limits times branching ratio on a Kaluza–Klein gluon decaying to $t\bar{t}$, combined samples. The observed and expected limits for each mass point are given, as well as the $\pm 1\sigma$ variation of the expected limit. The second column gives the theoretical predictions.

Mass (TeV)	$\sigma\times$ BR [pb]	Obs. (pb)	Exp. (pb)	-1σ (pb)	$+1\sigma$ (pb)
0.50	82.	9.62	6.73	2.15	14.1
0.60	45.	4.79	3.48	0.813	6.98
0.70	25.	3.48	1.84	0.436	3.90
0.80	15.	1.66	1.19	0.262	2.37
0.90	8.8	0.948	0.711	0.165	1.60
1.00	5.5	0.561	0.529	0.125	1.11
1.15	2.8	0.394	0.329	0.100	0.720
1.30	1.5	0.282	0.221	0.081	0.464
1.60	0.50	0.204	0.134	0.052	0.296
1.80	0.26	0.149	0.109	0.041	0.237
2.00	0.14	0.153	0.097	0.036	0.209
2.25	0.067	0.218	0.089	0.036	0.203
2.50	0.035	0.152	0.080	0.035	0.196

Table 5: Acceptance × efficiency for $Z' \to t\bar{t}$ samples.

Resolved selection acceptance × efficiency		
Z' mass [TeV]	e+jets	μ+jets
0.5	0.029 ± 0.0024	0.033 ± 0.0029
0.75	0.035 ± 0.0026	0.045 ± 0.004
1.0	0.031 ± 0.0025	0.039 ± 0.0029
1.25	0.0273 ± 0.0020	0.032 ± 0.0024
1.5	0.0247 ± 0.0016	0.029 ± 0.0018
1.75	0.0224 ± 0.0015	0.0255 ± 0.0017
2.0	0.0199 ± 0.0011	0.0255 ± 0.0018
2.25	0.0194 ± 0.0012	0.025 ± 0.0022
2.5	0.0183 ± 0.0011	0.0246 ± 0.0019
3.0	0.0194 ± 0.0011	0.0242 ± 0.0019
Boosted selection acceptance × efficiency		
Z' mass [TeV]	e+jets	μ+jets
0.5	0.00023 ± 0.00007	0.00011 ± 0.00004
0.75	0.0055 ± 0.0015	0.0063 ± 0.0020
1.0	0.0203 ± 0.0018	0.0272 ± 0.0023
1.25	0.0292 ± 0.0017	0.039 ± 0.0023
1.5	0.0313 ± 0.0022	0.046 ± 0.004
1.75	0.033 ± 0.004	0.050 ± 0.007
2.0	0.029 ± 0.005	0.053 ± 0.011
2.25	0.027 ± 0.006	0.051 ± 0.013
2.5	0.026 ± 0.006	0.051 ± 0.014
3.0	0.020 ± 0.004	0.045 ± 0.014

Table 6: Acceptance × efficiency for $g_{KK} \to t\bar{t}$ samples.

Resolved selection acceptance × efficiency		
g_{KK} mass [TeV]	e+jets	μ+jets
0.5	0.0277 ± 0.0021	0.0351 ± 0.0029
0.6	0.0327 ± 0.0025	0.0400 ± 0.0032
0.7	0.0340 ± 0.0025	0.0440 ± 0.0032
0.8	0.0350 ± 0.0028	0.0437 ± 0.0035
0.9	0.0313 ± 0.0024	0.0400 ± 0.0032
1.0	0.0300 ± 0.0023	0.0370 ± 0.0028
1.15	0.0281 ± 0.0019	0.0355 ± 0.0024
1.30	0.0256 ± 0.0020	0.0344 ± 0.0024
1.6	0.0253 ± 0.0016	0.0304 ± 0.0018
1.8	0.0230 ± 0.0014	0.0289 ± 0.0017
2.0	0.0229 ± 0.0012	0.0286 ± 0.0017
2.25	0.0218 ± 0.0015	0.0287 ± 0.0016
2.5	0.0223 ± 0.0013	0.0293 ± 0.0017
Boosted selection acceptance × efficiency		
g_{KK} mass [TeV]	e+jets	μ+jets
0.5	0.00037 ± 0.00009	0.00042 ± 0.00008
0.6	0.00107 ± 0.00023	0.00122 ± 0.00030
0.7	0.0030 ± 0.0008	0.0039 ± 0.0011
0.8	0.0085 ± 0.0016	0.0104 ± 0.0020
0.9	0.0143 ± 0.0016	0.0170 ± 0.0022
1.0	0.0180 ± 0.0017	0.0242 ± 0.0022
1.15	0.0233 ± 0.0014	0.0298 ± 0.0020
1.30	0.0259 ± 0.0015	0.348 ± 0.0021
1.6	0.0288 ± 0.0020	0.039 ± 0.004
1.8	0.0277 ± 0.0027	0.042 ± 0.005
2.0	0.026 ± 0.004	0.041 ± 0.007
2.25	0.0241 ± 0.0034	0.039 ± 0.007
2.5	0.0210 ± 0.0031	0.038 ± 0.008

Same-sign dilepton analysis

VLQ branching ratios

Table: VLQ branching fractions (in percent) for masses near the limit of our sensitivity, assuming the singlet and doublet models of arXiv:0907.3155 [hep-ph].

	B			T		
Mass (model)	Wt	Zb	Hb	Wb	Zt	Ht
0.50 TeV (singlet)	42	31	27	50	17	33
0.50 TeV (doublet)	100	0	0	0	34	66
0.55 TeV (singlet)	43	30	27	49	18	32
0.55 TeV (doublet)	100	0	0	0	37	63
0.60 TeV (singlet)	44	29	26	49	19	31
0.60 TeV (doublet)	100	0	0	0	38	62
0.65 TeV (singlet)	45	29	26	49	20	30
0.65 TeV (doublet)	100	0	0	0	40	60

Limits on VLQ mass @ 95% C.L. (same-sign analysis)

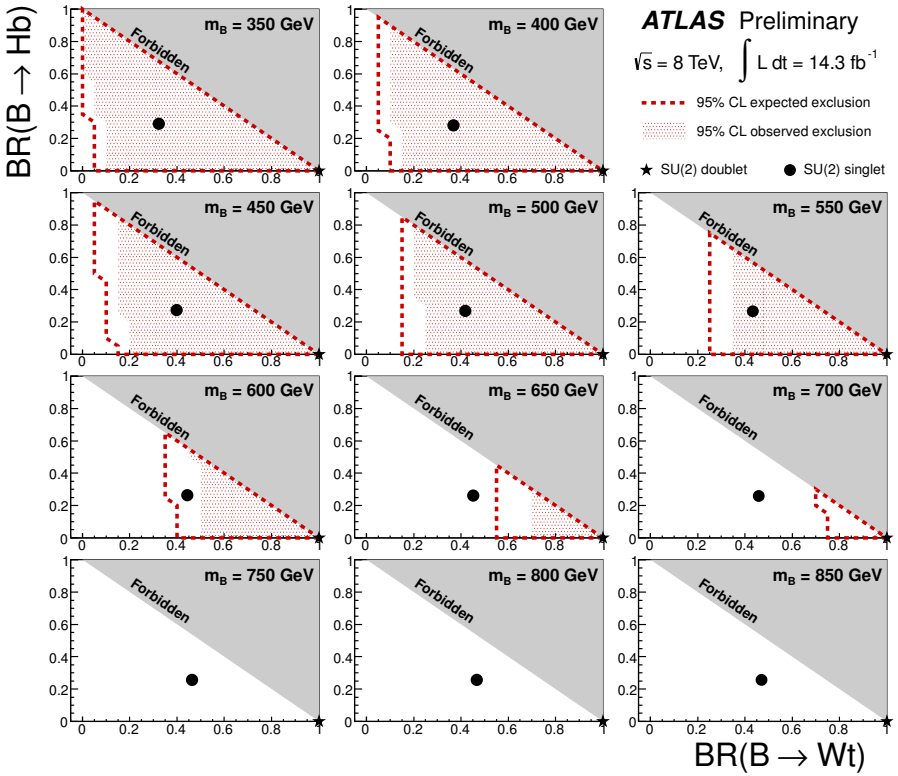

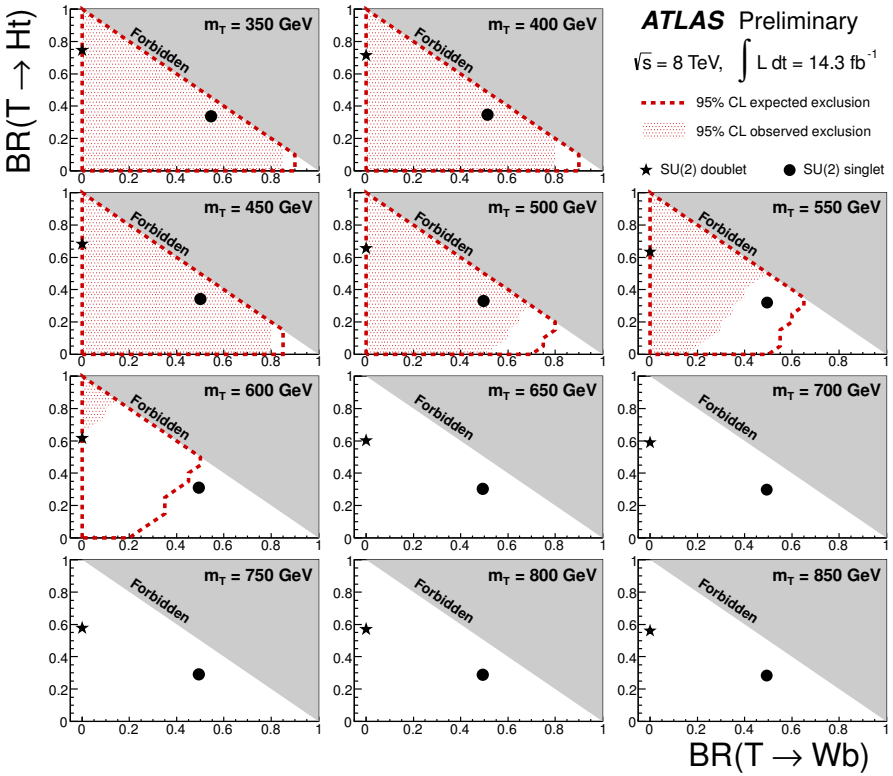

Discriminant variables: $e\mu$

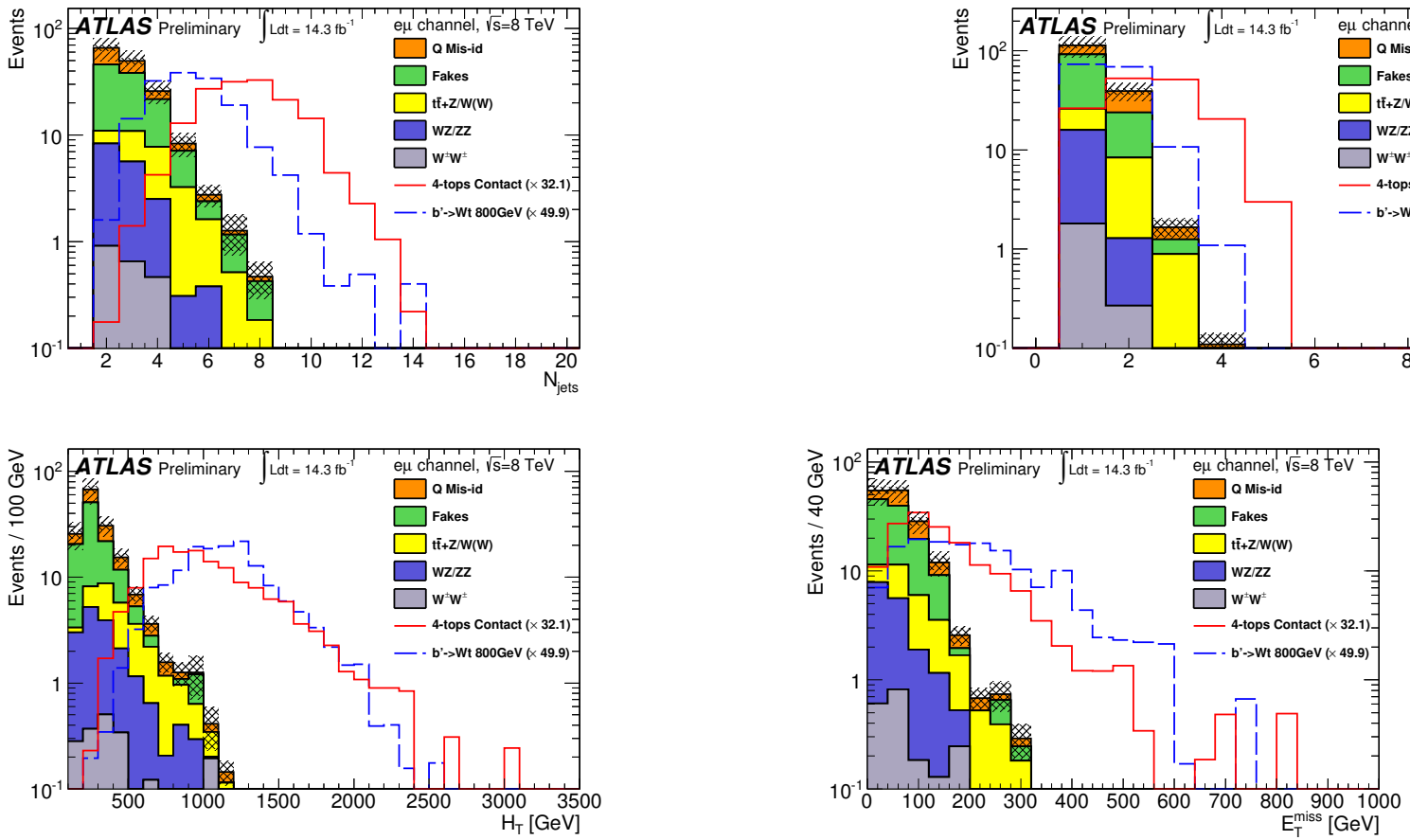

Figure: Distributions of discriminant variables in the $e\mu$ channel, after the standard object selection and with the requirement that $E_T^{miss} > 40$ GeV. The assumed strength of the contact interaction is $C/\Lambda^2 = -4\pi\, TeV^{-2}$.

Mis-id rates of the electron charge and overlap with fakes

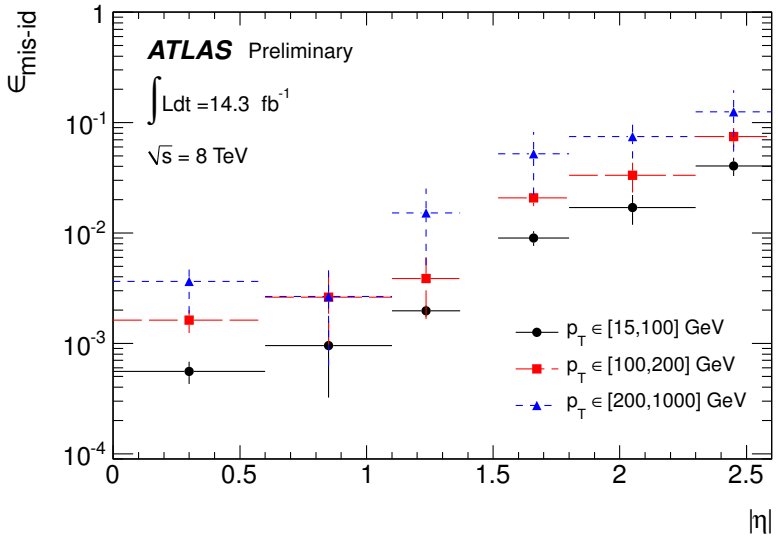

(a)

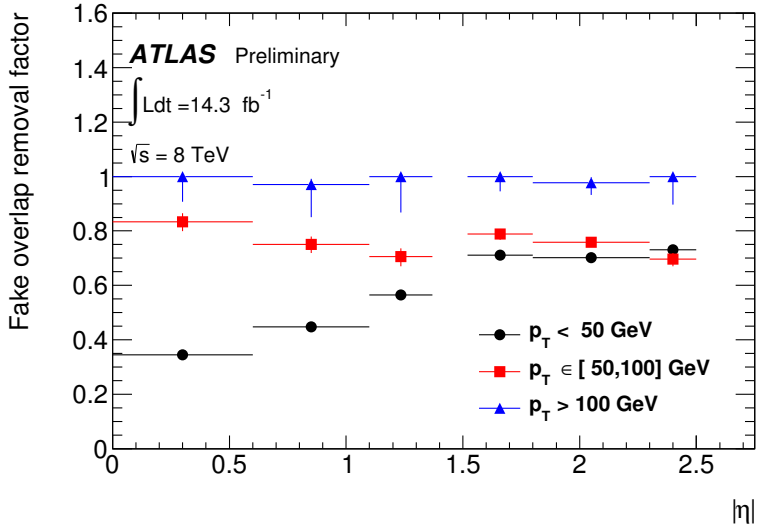

(b)

Control region: 100 GeV $< H_T <$ 400 GeV

Samples	Channel		
	ee	$e\mu$	$\mu\mu$
Charge misidentification	$25.7 \pm 0.7 \pm 6.6$	$30.2 \pm 0.6 \pm 7.9$	—
Fakes	$38.7 \pm 3.7 \pm 11.6$	$73.1 \pm 5.3 \pm 21.9$	$33.4 \pm 8.5 \pm 10.0$
Diboson			
• WZ/ZZ+jets	$3.9 \pm 0.7 \pm 1.3$	$10.9 \pm 1.2 \pm 3.7$	$5.1 \pm 0.8 \pm 1.7$
• $W^{\pm}W^{\pm}$+2 jets	$0.4 \pm 0.2 \pm 0.2$	$1.2 \pm 0.3 \pm 0.6$	$0.8 \pm 0.2 \pm 0.4$
$t\bar{t} + W/Z$			
• $t\bar{t}W$(+jet)	$1.7 \pm 0.1 \pm 0.5$	$6.6 \pm 0.2 \pm 2.0$	$4.3 \pm 0.2 \pm 1.3$
• $t\bar{t}Z$(+jet)	$0.5 \pm 0.1 \pm 0.1$	$1.5 \pm 0.1 \pm 0.5$	$0.8 \pm 0.1 \pm 0.2$
• $t\bar{t}W^+W^-$	0.014 ± 0.002	0.050 ± 0.004	0.029 ± 0.003
Total expected background	$71 \pm 5 \pm 13$	$124 \pm 8 \pm 24$	$44 \pm 11 \pm 10$
Observed	64	97	38
Signal contamination			
• $b' \rightarrow Wt$ (800 GeV)	< 0.003	0.009 ± 0.006	0.002 ± 0.001
• 4 tops contact ($C/\Lambda^2 = -4\pi TeV^{-2}$)	0.009 ± 0.005	0.06 ± 0.02	0.02 ± 0.01

Systematic uncertainties

	Uncertainty in %					
	650 GeV b'			Background		
Source	ee	$e\mu$	$\mu\mu$	ee	$e\mu$	$\mu\mu$
Cross section	–	–	–	14.4	25.4	32.9
Fakes	–	–	–	9.7	1.4	10.1
Charge misidentification	–	–	–	7.2	7.1	–
Jet energy scale	4.6	2.5	0.2	3.5	10.2	4.4
ISR/FSR	6.0	6.0	6.0	2.6	4.5	4.0
b-tagging efficiency	4.6	3.1	3.0	2.1	4.4	4.0
Lepton ID efficiency	5.3	4.9	8.2	2.2	3.6	5.4
Jet energy resolution	0.8	0.9	0.3	0.9	2.7	2.0
Luminosity	3.6	3.6	3.6	1.6	2.7	3.6
Lepton energy scale	0.8	0.4	0.0	1.4	0.9	0.1
JVF selection efficiency	2.5	2.9	2.6	1.1	1.5	1.4

Data and expected background: $e\mu$ channel

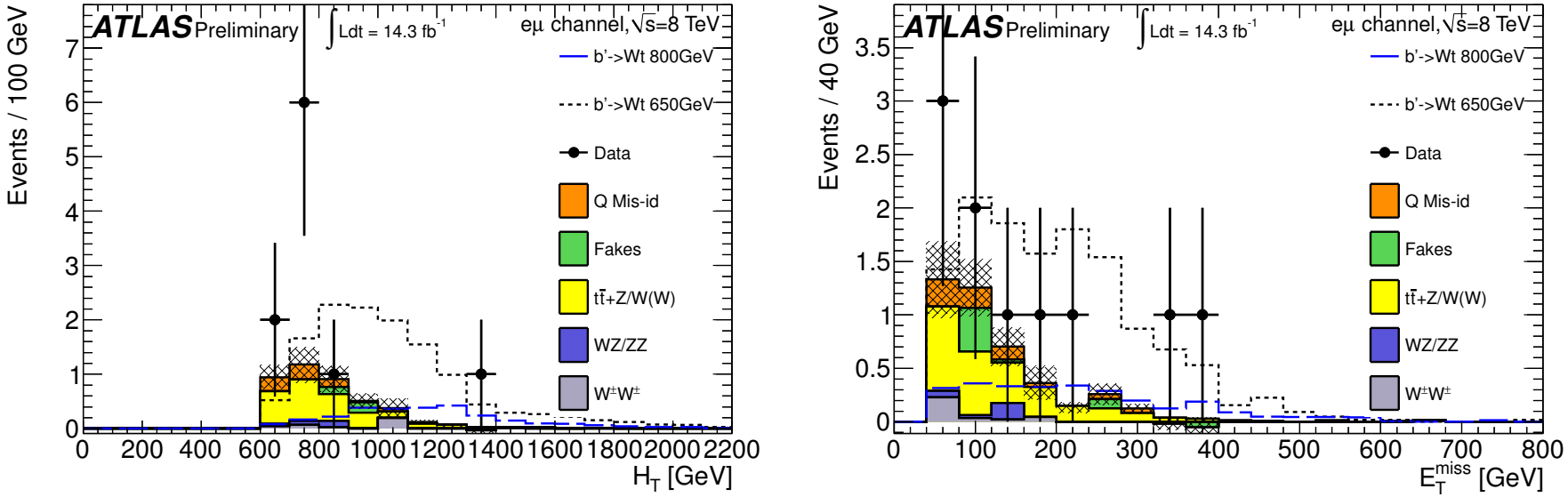

Discriminant variables after VLQ/b' selection

Data and expected background: $\mu\mu$ channel

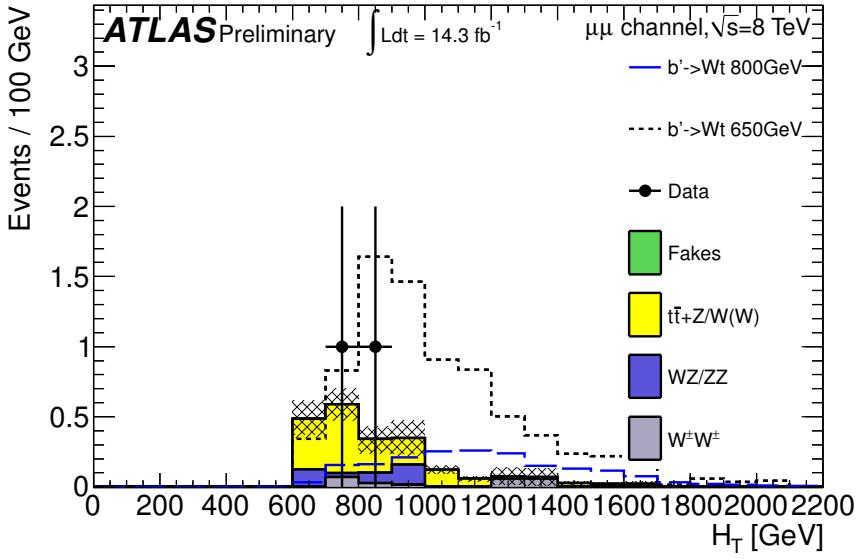

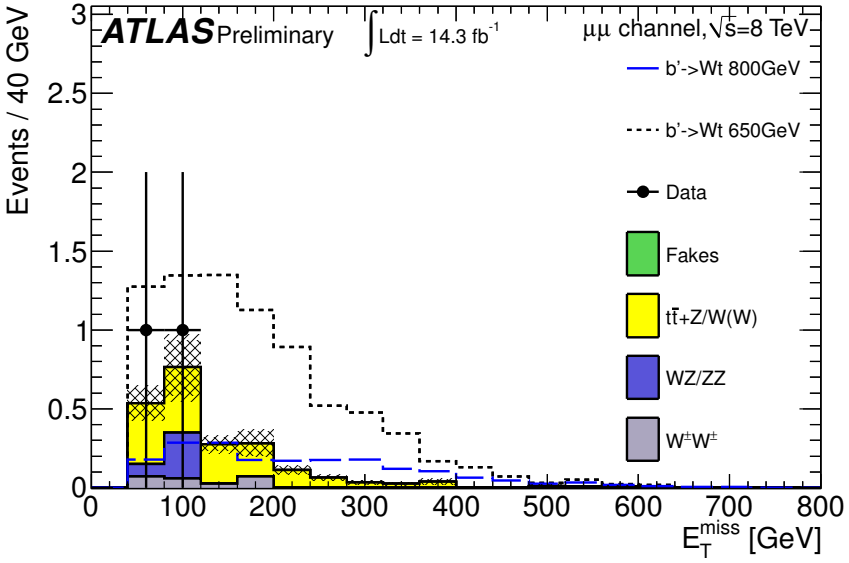

Discriminant variables after VLQ/b' selection

Table: Observed and expected number of events with statistical (first) and systematic (second) uncertainties for the b'/VLQ signal selection.

Backgrounds	Channel		
Samples	ee	$e\mu$	$\mu\mu$
Charge misidentification	$0.6 \pm 0.1 \pm 0.2$	$0.9 \pm 0.1 \pm 0.3$	—
Fakes	$0.8 \pm 0.4 \pm 0.3$	$0.2 \pm 0.4 \pm 0.1$	< 1.1
Diboson			
• WZ/ZZ+jets	$0.3 \pm 0.2 \pm 0.1$	$0.3 \pm 0.1^{+0.4}_{-0.2}$	$0.4 \pm 0.2 \pm 0.1$
• $W^{\pm}W^{\pm}$+2 jets	$0.17 \pm 0.09 \pm 0.05$	$0.3 \pm 0.2 \pm 0.1$	$0.2 \pm 0.1 \pm 0.1$
$t\bar{t} + W/Z$			
• $t\bar{t}W$(+jet(s))	$0.6 \pm 0.2 \pm 0.3$	$1.9 \pm 0.2 \pm 0.6$	$1.3 \pm 0.2 \pm 0.4$
• $t\bar{t}Z$(+jet(s))	$0.18 \pm 0.03 \pm 0.06$	$0.66 \pm 0.05 \pm 0.22$	$0.31 \pm 0.04 \pm 0.10$
• $t\bar{t}W^+W^-$	$0.024 \pm 0.003^{+0.010}_{-0.007}$	$0.072 \pm 0.005^{+0.028}_{-0.020}$	$0.055 \pm 0.004^{+0.022}_{-0.016}$
Total expected background	$2.7 \pm 0.5 \pm 0.4$	$4.4 \pm 0.5^{+0.9}_{-0.7}$	$2.3 \pm 1.2 \pm 0.5$
Observed	3	10	2

Table: Observed and expected number of events with statistical (first) and systematic (second) uncertainties for the positively-charged top pair signal selection.

Samples	Channel		
	ee	$e\mu$	$\mu\mu$
Charge misidentification	$0.6 \pm 0.1 \pm 0.2$	$0.5 \pm 0.1 \pm 0.2$	—
Fakes	$0.6 \pm 0.4 \pm 0.2$	$1.0 \pm 0.4 \pm 0.3$	$0.7 \pm 0.7 \pm 0.2$
Diboson			
• WZ/ZZ+jets	$0.2 \pm 0.1 \pm 0.1$	$0.5 \pm 0.3 \pm 0.2$	$0.6 \pm 0.3 \pm 0.2$
• $W^{\pm}W^{\pm}$+2 jets	$0.16 \pm 0.08 \pm 0.04$	$0.3 \pm 0.2 \pm 0.1$	$0.2 \pm 0.1 \pm 0.1$
$t\bar{t} + W/Z$			
• $t\bar{t}W$(+jet(s))	$0.7 \pm 0.1 \pm 0.2$	$2.2 \pm 0.1 \pm 0.7$	$1.5 \pm 0.1 \pm 0.5$
• $t\bar{t}Z$(+jet(s))	$0.18 \pm 0.03 \pm 0.06$	$0.59 \pm 0.05 \pm 0.19$	$0.26 \pm 0.03 \pm 0.09$
• $t\bar{t}W^{+}W^{-}$	$0.013 \pm 0.002 \pm 0.005$	$0.053 \pm 0.004 \pm 0.021$	$0.032 \pm 0.003 \pm 0.013$
Total	$2.5 \pm 0.4 \pm 0.4$	$5.1 \pm 0.5 \pm 0.9$	$3.3 \pm 0.8 \pm 0.7$
Observed	3	8	1

Table: Observed and expected number of events with statistical (first) and systematic (second) uncertainties for the four top quarks signal selection.

Samples	Channel		
	ee	$e\mu$	$\mu\mu$
Charge misidentification	$0.16 \pm 0.04 \pm 0.05$	$0.41 \pm 0.07 \pm 0.12$	—
Fakes	$0.18 \pm 0.17 \pm 0.05$	$0.07 \pm 0.28 \pm 0.02$	< 1.14
Diboson			
• WZ/ZZ+jets	< 0.1	$0.01 \pm 0.09 \pm 0.01$	< 0.11
• $W^{\pm}W^{\pm}$+2 jets	< 0.03	$0.18 \pm 0.16 \pm 0.07$	< 0.03
$t\bar{t} + W/Z$			
• $t\bar{t}W$(+jet(s))	$0.31 \pm 0.04 \pm 0.12$	$0.93 \pm 0.06 \pm 0.35$	$0.65 \pm 0.06 \pm 0.25$
• $t\bar{t}Z$(+jet(s))	$0.09 \pm 0.02 \pm 0.04$	$0.34 \pm 0.04 \pm 0.14$	$0.14 \pm 0.02 \pm 0.06$
• $t\bar{t}W^{+}W^{-}$	$0.012 \pm 0.002 \pm 0.005$	$0.039 \pm 0.003 \pm 0.016$	$0.024 \pm 0.003 \pm 0.01$
Total	$0.8 \pm 0.2 \pm 0.1$	$2.0 \pm 0.4 \pm 0.4$	$0.8 \pm 1.2 \pm 0.3$
Observed	1	6	1

Table: Event selection efficiencies (in percent), relative to the inclusive cross section for the $b' \to Wt$ and $b' \to Wq$ ($\sim 1/3$ for each $q = u, c, t$) signals, for several generated mass points. They are computed with respect to the generated events passing the lepton filter, and where the W is free to decay hadronically or leptonically.

Process	Channel		
	ee	$e\mu$	$\mu\mu$
$b'(400GeV) \to Wt$	0.11 ± 0.01	0.39 ± 0.02	0.25 ± 0.02
$b'(600GeV) \to Wt$	0.30 ± 0.02	0.82 ± 0.03	0.53 ± 0.02
$b'(800GeV) \to Wt$	0.37 ± 0.02	1.02 ± 0.03	0.64 ± 0.02
$b'(1000GeV) \to Wt$	0.35 ± 0.02	1.11 ± 0.03	0.63 ± 0.02
$b'(400GeV) \to Wq$	0.024 ± 0.004	0.082 ± 0.007	0.060 ± 0.006
$b'(600GeV) \to Wq$	0.09 ± 0.01	0.25 ± 0.01	0.14 ± 0.01
$b'(800GeV) \to Wq$	0.13 ± 0.01	0.32 ± 0.01	0.19 ± 0.01
$b'(100GeV) \to Wq$	0.10 ± 0.01	0.32 ± 0.02	0.20 ± 0.01

Table: Event selection efficiencies (in percent), relative to the inclusive cross section for the vector-like T (B) signal for several generated T (B) mass points. Efficiencies are computed assuming the branching ratios from the singlet model.

Process	Channel		
	ee	$e\mu$	$\mu\mu$
TT (350 GeV)	0.013 ± 0.002	0.038 ± 0.003	0.024 ± 0.003
TT (550 GeV)	0.055 ± 0.004	0.136 ± 0.006	0.082 ± 0.005
TT (750 GeV)	0.065 ± 0.005	0.176 ± 0.008	0.080 ± 0.005
TT (850 GeV)	0.065 ± 0.005	0.171 ± 0.007	0.093 ± 0.005
BB (350 GeV)	0.011 ± 0.002	0.043 ± 0.004	0.024 ± 0.003
BB (550 GeV)	0.068 ± 0.005	0.218 ± 0.008	0.129 ± 0.006
BB (750 GeV)	0.098 ± 0.006	0.269 ± 0.009	0.185 ± 0.008
BB (850 GeV)	0.128 ± 0.006	0.344 ± 0.010	0.191 ± 0.008

Table: Event selection efficiencies (in percent), relative to the dileptonic cross section (both W bosons must decay to e, μ or τ), for the positively-charged top pair signal.

Process	Channel		
	ee	$e\mu$	$\mu\mu$
Left-left	0.48 ± 0.02	1.59 ± 0.04	1.27 ± 0.04
Left-right	0.41 ± 0.02	1.46 ± 0.04	1.19 ± 0.03
Right-right	0.40 ± 0.02	1.42 ± 0.04	1.14 ± 0.03

Table: Event selection efficiencies (in percent), relative to the inclusive cross section, for the four top quarks signals (all decay modes of the W are included).

Process	Channel		
	ee	$e\mu$	$\mu\mu$
Standard Model	0.11 ± 0.01	0.39 ± 0.01	0.28 ± 0.01
Contact interaction	0.15 ± 0.01	0.53 ± 0.02	0.41 ± 0.02
Sgluon (350 GeV)	0.03 ± 0.01	0.09 ± 0.01	0.07 ± 0.01
Sgluon (400 GeV)	0.06 ± 0.01	0.17 ± 0.02	0.13 ± 0.02
Sgluon (500 GeV)	0.13 ± 0.02	0.47 ± 0.03	0.23 ± 0.02
Sgluon (600 GeV)	0.15 ± 0.02	0.61 ± 0.04	0.41 ± 0.03
Sgluon (800 GeV)	0.20 ± 0.02	0.75 ± 0.04	0.48 ± 0.03
Sgluon (1000 GeV)	0.16 ± 0.02	0.57 ± 0.03	0.49 ± 0.03
2UED/RPP (600 GeV)	0.26 ± 0.01	0.93 ± 0.02	0.66 ± 0.02
2UED/RPP (800 GeV)	0.25 ± 0.01	0.88 ± 0.02	0.67 ± 0.02
2UED/RPP (1000 GeV)	0.23 ± 0.01	0.85 ± 0.02	0.67 ± 0.02
2UED/RPP (1200 GeV)	0.22 ± 0.01	0.88 ± 0.02	0.67 ± 0.02

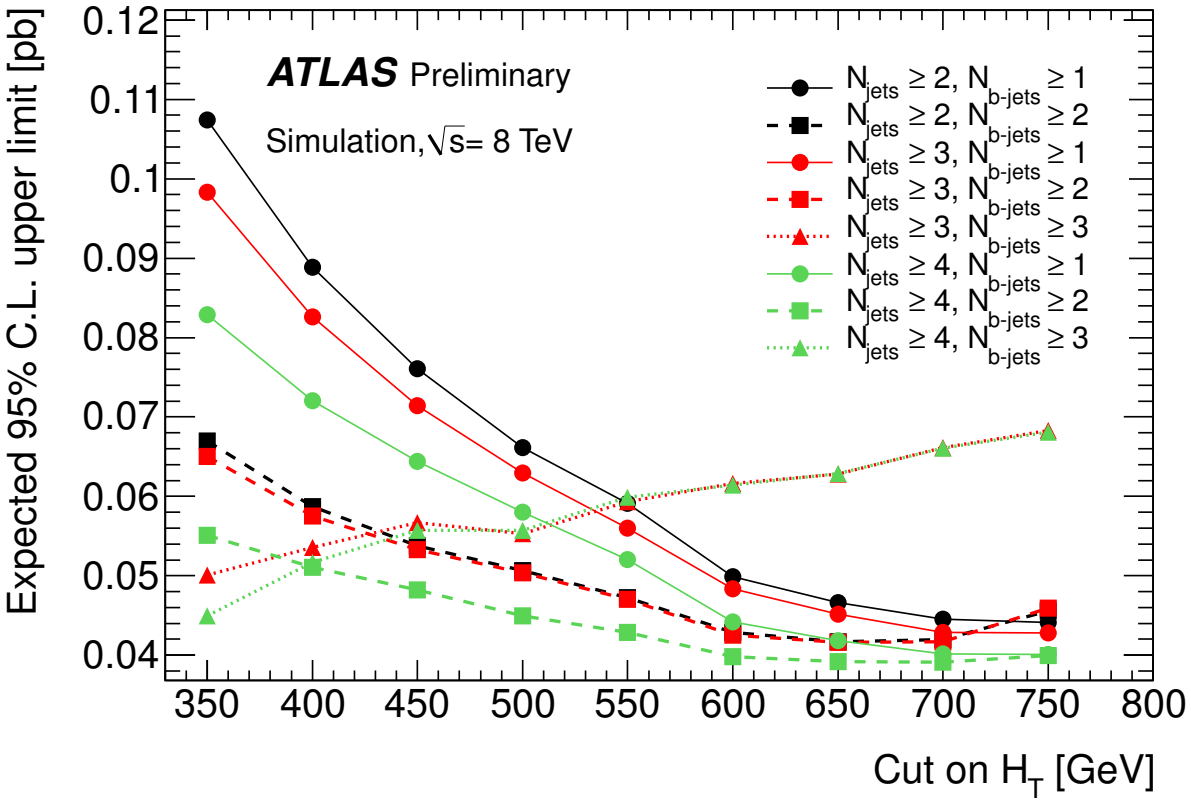

Figure: Expected 95% C.L. upper limit on the four tops contact interaction production cross section as a function of the cut on H_T, and parametrized with the requirement on the number of jets (different colors), and on the number of b-jets (different markers). The final event selection is chosen so that it can provide the minimum value on the cross-section. Following the information provided by this plot, the best choice for the final selection is $H_T \geq 650$ GeV, $\mathrm{N_{jets}} \geq 2$ and $\mathrm{N_{b-jets}} \geq 2$.

Previous results

Exclusion ranges @ 95% C.L:

1. **ATLAS (4.7 fb^{-1} @ 7 TeV) ATLAS-CONF-2012-136:** 0.5 TeV $< m_{Z'} <$ 1.7 TeV.
2. **ATLAS (4.7 fb^{-1} @ 7 TeV) ATLAS-CONF-2012-136:** $0.5 < g_{KK} <$ 1.9 TeV
3. **ATLAS (4.7 fb^{-1} @ 7 TeV):** $m_{b'} <$ 0.67 TeV if BR($b' \to Wt$)=1 ATLAS-CONF-2012-130.
4. **ATLAS (1.04 fb^{-1} @ 7 TeV):** $\sigma(pp \to tt) >$ 1.7 pb arXiv:1202.5520 [hep-ex].
5. **ATLAS (4.7 fb^{-1} @ 7 TeV):** $\sigma(pp \to t\bar{t}t\bar{t}) >$ 61 fb ATLAS-CONF-2012-130.